Reprinted from

Journal of
APPLIED PHYSICS

Volume 74 15 December 1993 Number 12

Theory of the electron fracture mode in solids

Genady P. Cherepanov
College of Engineering and Design, Florida International University, Miami, Florida 33199

Andrew A. Borzykh
Kursk Polytechnic Institute, Kursk, Russia, CIS

pp. 7134-7153

a publication of the American Institute of Physics

AIP

Theory of the electron fracture mode in solids

Genady P. Cherepanov[a)]
College of Engineering and Design, Florida International University, Miami, Florida 33199

Andrew A. Borzykh
Kursk Polytechnic Institute, Kursk, Russia, CIS

(Received 11 January 1993; accepted for publication 26 August 1993)

The theoretical model serving to explain and describe the phenomenon of the electron fracture mode (EFM) discovered experimentally nearly 20 years ago is advanced. EFM is characterized by the brittle cleavage of common plastic crystals proceeding with supersonic velocities independently of initial cracks when subjected to high-intensity electron beams. Using the invariant Γ integral of an electromagnetic deformable medium, it is proven that two electrons moving faster than the phase speed of light attract one another, as distinct from the common Coulomb's law. Self-packing of such relativistic electron beams is studied using a periodic chain model. It is suggested that during irradiation of a solid by a high-intensity electron beam, some electron clusters are formed, which act as wedges cutting the crystalline specimen. The dynamic problem of supersonic cutting by a thin wedge is studied, and the drag is calculated. The length of the resulting crack is computed. The theoretical results are confirmed by available experimental data.

I. INTRODUCTION

In the mid 1960s, high-power pulse electron-beam accelerators having a voltage of some millions of volts were invented and later used to fracture various materials. Experimental data analysis enabled discovery of a new mode of fracture in several ductile crystals caused by a specific energy supply to the crack tip. The mode differs from the well-known thermomechanical modes of fracture caused by the "heat-thermostress-crack" mechanism. We call this new mode the electron fracture mode (EFM). It is characterized by the following three special features: (i) Initial macrocracks in a specimen do not affect the threshold of fracture; in other words, the value of the beam intensity at which the specimen breaks; (ii) fracture of different materials, which can be very ductile under usual mechanical loads, occurs in a brittle manner; that is, the specimen usually splits by a crack without any residual deformations; (iii) the splitting cracks propagate with supersonic velocities. These data are controversial from the point of view of fracture mechanics and, hence, they cannot be understood or explained with traditional theories.

The purpose of the present study is to create a simple practical model of the EFM. Our basic viewpoint can be briefly summarized as follows: During irradiation of a solid by a high-intensity electron beam, some electron clusters are formed and act as "blades" or "wedges," cutting the crystalline specimen.

In this section, experimental data on the EFM are analyzed and discussed, while the peculiarities of the EFM are specified. As a result, we can conclude that the processes caused by the EFM are unusual from the point of view of common fracture mechanics.

In Sec. II, the invariant Γ integrals of an electromagnetic deformable medium are modified for supersonic singularities. The basic model and some problems explaining and describing the EFM are formulated.

In Sec. III the relativistic electron interactions in beams are considered. Using Γ integrals, we derive the law of the interaction of two moving relativistic charges; that is, the generalized Coulomb's law for relativistic charges. In particular, when two relativistic electrons e move with the same velocity v, one behind the other along a rectilinear trajectory, the force F acting upon the rear electron is equal to

$$F=\frac{e^2}{2\pi\epsilon' R^2}\frac{(v^2/a^2)-1}{1-(v^2/c^2)}, \quad \text{where } a=\frac{c}{\sqrt{\mu\epsilon}}.$$

Here R is the distance between the electrons, c is the speed of light in vacuum, and a is the phase speed of light in a medium having electromagnetic constants, μ, ϵ, and ϵ'. It appears that two electrons moving faster than the phase speed of light attract each other, as distinct from the common Coulomb's law; hence, the beams of such relativistic electrons tend to self-pack and self-compress. The latter problem is studied using a periodic chain model of the electron beam.

In Sec. IV the dynamic elastic problem of supersonic cutting by a thin wedge is formulated and solved, and the drag force is calculated.

In Sec. V the problem of deceleration of the moving wedge is solved in quasisteady approximation. The length of a resulting cut, that is, the final crack, is determined. Some applications of the analytical solutions are given.

In Sec. VI the theoretical results are analyzed and compared with experimental results. The role of relativistic electrons is estimated and some parameters of solid-state electron clusters are defined.

The necessity of further study of this mysterious phenomenon is emphasized in Sec. VII.

[a)]Formerly at Division of Applied Sciences, Harvard University, Cambridge, MA 02138.

 0021-8979/93/74(12)/7134/20/$6.00

A. Principal characteristics of the means of fracture and experimental conditions

In the 1960s, investigation of the fracture of solids by beams of electrons and other particles was connected with the creation of powerful sources of such radiation, for example, accelerators using shock autoemission from a pointed cathode in strong electric fields. The first results of the fracture of Si, Ge, InSb semiconductor crystals by high-energy electron beams were published[1] by Oswald in 1966. In the works that followed, one can also find some investigations of the fracture of certain metals;[2–9] certain dielectrics;[10–12] ionic crystals;[13–22] inorganic glass;[23,24] and rocks.[25–28] In Russia, most of the investigations were done in the 1970s, and later the work in this area was classified.

Irradiation of the materials investigated in fracture experiments was done by nanosecond pulses of homogeneous electron beams with a pulse span 1 ns to 1 μs. The average kinetic energy of a single electron in the beam was equal to $E_e \sim 0.1$–15 MeV. For reference, the chemical bond energy in solids is of the order of 1 eV. The beam intensity was measured within the limits from 10^{22} to 10^{27} s^{-1} m^{-2} (current density, 10^3–10^8 A/m^2) so that the average particle density Φ equals 10^{14}–10^{19} particles/m^2. The pulse radiation frequency reached 360 cycles per second. It is significant that for these energies electrons in the beam are relativistic. The relationship between energy E and the velocity of a particle v in relativistic mechanics has the form

$$E=\frac{m_0c^2}{\sqrt{1-v^2/c^2}}-m_0c^2, \tag{1.1.1}$$

where m_0 is the mass of the particle at rest, and c is the velocity of light in a vacuum. Thus,

$$\frac{v}{c}=\sqrt{1-(1+E_*)^{-2}}, \quad E_*=\frac{E}{m_0c^2}.$$

For instance, for an electron with energy E of 0.5 MeV, we get $v/c \simeq 0.85$, $c/v \simeq 1.18$, and $v \simeq 0.25$ Gm/s. This velocity exceeds the phase speed of light in a number of media, e.g., for many dielectrics. And the scattering of particle velocities in the beam ensures the presence of superluminal electrons for even smaller energies of a beam.[29] The dependence in Eq. (1.1.1) is shown in Fig. 1. Superluminal electrons are electrons moving in a medium with a speed exceeding the phase velocity of light.

Note that for energies of about 1 MeV, relativistic effects are essential for light particles only (for electrons, $m_0c^2 \simeq 0.5$ MeV, and for neutrons and protons, $m_0c^2 \simeq 0.94$ GeV), and that further increase of energy changes the particle velocity only insignificantly, bringing it closer to the velocity of light in the vacuum c.

The average distance between the particles in the beam can be estimated, according to the data mentioned above, about 1–10 μm (in the laboratory system of coordinates of the observer, since with the velocities approaching that of light, relativistic effects begin to play a role). Substituting these values into Heisenberg's uncertainty principle, namely 1 MeV for ΔE and 10^{-3} ps for Δt, we obtain

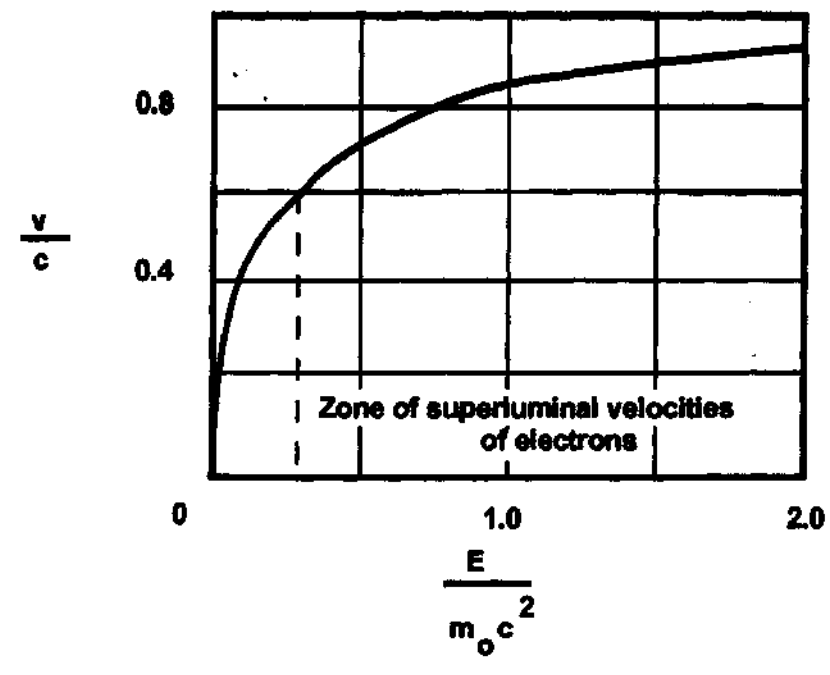

FIG. 1. Dependence of the velocity of a particle v on its energy E.

$$\Delta E \Delta t = 10^{-27} \text{ J s} \gg \hbar. \tag{1.1.2}$$

Hence interactions of particles in the beam are of a nonquantum character, and the electrons can be considered material particles having no dimensions. The quantum character of the interaction between the electrons of such energies arises at distances of the order of 10^{-1} pm (the dimension of the electron localization region, according to the uncertainty principle).

Let us also dwell upon the question of the character of the interaction between radiation and the material exposed to radiation. The totality of atomic nuclei forming the structure of the substance, and the electrons, take up an insignificantly small volume in comparison with the volume of the solid they form. Interatomic distances have the order of 10^{-1} nm (e.g., for NaCl, the lattice spacing, $a=0.5$ nm), the radius of the nucleus, 10^{-14} m, and the classic radius of the electron is of the order 2.8×10^{-15} m. Since the electron density in a solid is of the same order as that of atoms in the case of the electron radiation considered, the irradiated material can be regarded as a continuum. Evaluating the character of the interaction of the beam particles with the nucleons of the solid, with the help of Eq. (1.1.2), we shall find that this interaction can also be considered nonquantum.

In order to eliminate additional mechanical effects, the dimensions of the irradiated samples in the fracture experiments were such that the absorbed energy was homogeneous for the sample volume. The qualitative pattern of distribution of specific absorbed energy W within sample thickness h_s is presented[30] in Fig. 2.

The value h_0 is the range of a particle in a substance (e.g., for NaCl, $h_0=0.45$ mm). From Fig. 2, one can see that the requirement of homogeneity is fulfilled approximately with the sample thickness, $h_s \sim h_0/2$. In the experiments the thickness of the samples varied from 0.05 mm to some millimeters (for metals); while investigating the influence of the inhomogeneity of the absorbed energy, the sample thickness exceeded the values mentioned to a great extent. Other sample dimensions were usually restricted by the dimensions of the homogeneous beam of the particles; in high-voltage accelerators, the beam radius was several

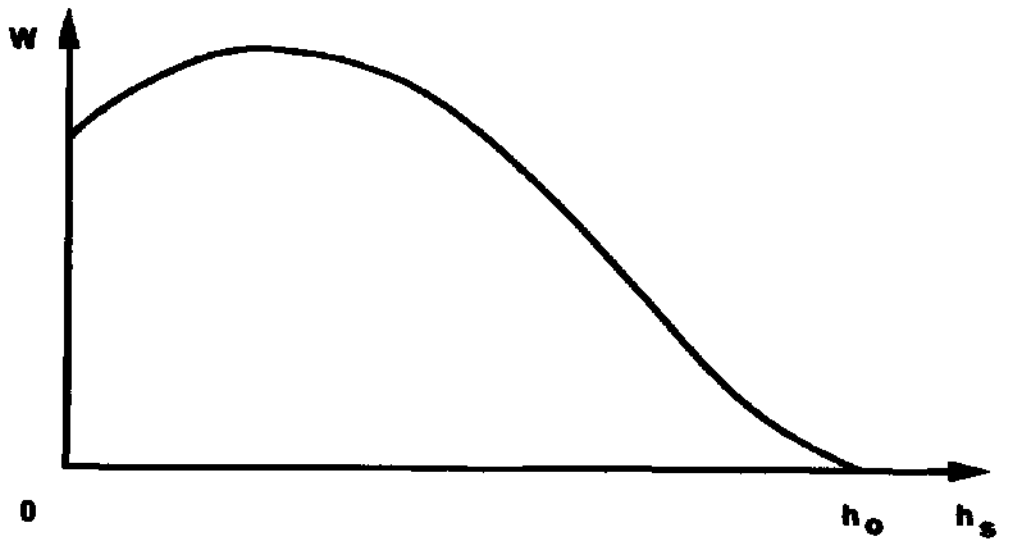

FIG. 2. Qualitative dependence of the specific absorbed energy W on the sample thickness h_s.

millimeters. Under laboratory conditions, the accelerator and the samples investigated were placed in a vacuum chamber to reduce energy losses. The materials investigated also included strong, defect-free whisker crystals and radiation-hardened materials whose mechanical properties differ greatly from those of common materials.[16]

The average absorbed specific energy during irradiation, $W=10^{-1}$–10 eV/nm^3 (10^{-2}–1 GJ/m^3), while threshold fracture energies were of the order of 10^{-1} eV/nm^3. The critical values of $W=W_c$ for some materials are presented in Table I. The quantities W_c are two or three orders less than the binding energy of ideal crystals (for NaCl, according to Ref. 31, the binding energy $U_c=400$ eV/nm^3, i.e., 75 GJ/m^3), i.e., the theoretical strength of the material.

TABLE I. Thresholds of irradiation power and fracture energy for some materials.

Materials	Φ_c (W/nm^2)	W_c (eV/nm^3)	Ref.
RbCl	0.09	0.12	15
ZnS	0.36	0.14	15
InSb	0.17	0.50	1
Si	0.50	2.05	1
LiF	0.17	0.24	15
	0.17	0.30	18
NaF	0.13	0.18	15
	0.13	0.23	18
NaCl	0.11	0.14	15
	0.11	0.20	18
Ge	0.3	1.20	15
	0.3	1.50	18
	0.3	1.17	1
Al	0.67	...	40
KBr	0.09	0.12	15
Whisker crystal KBr	0.42	0.57	15
KCl	0.07	0.11	18
	0.08	0.09	19
	0.07	0.09	15
Whisker crystal KCl	0.42	0.47	15
Rocks[a]	...	450–750[b]	25,26

[a]Basalt, granite, sandstone, limestone, greenstone, marble, and clayey schist were studied.
[b]Specific absorbed energy of irradiation ensuring fracture.

B. Influence of irradiation by high-power electron beams on solids (experimental data)

When solids are irradiated by powerful pulse beams of relativistic electrons, a number of specific mechanical and physical phenomena appear. Let us mention the main effects. Fracture of various materials, even those that are very ductile under usual conditions, occurs in a "brittle" way.[1,4,7,14,15] Fracture is of a threshold nature characterized by the absence of accumulation effects and determined by the value of the critical density irradiation or by the corresponding density of absorbed energy.[1,15,24,32–36] Cracks fracturing the sample grow with super-Rayleigh and supersonic velocities.[15,19,26,37,38] Macrodefects and preliminary man-made cracks have negligible influence on the fracture of dielectrics.[15,21,35,39] Thresholds of fracture depend slightly on the temperature and purity of crystals and also on the energy of relativistic particles.[15,23,36] In an ultrashort range (10^{-1}–10 ps), the conductance of dielectrics grows many times.[11,21] Dielectrics glow in ultraviolet and visible spectral regions.[19] Powerful electron emissions turn into a vacuum discharge between the surface of the dielectric and the anode.[16] We will consider these peculiarities in more detail below.

First, we shall consider the fracture of samples with small thicknesses for which the absorbed energy distribution can be regarded as close to homogeneous. All of the materials are characterized by brittle fracture of the samples along one or two main cracks; in fact, any effects of ductility, even for metals, are not observed at all.[7,40,41] The second characteristic feature comprises low fracture thresholds for specific absorbed energy W_c (or the density of irradiation Φ_c). The values W_c and Φ_c, for some materials are shown in Table I. If the beam intensity exceeds the threshold value ($\Phi>\Phi_c$), a single pulse can produce fracture. Fracture accumulation at precritical irradiation is very weak; when $\Phi=0.7\Phi_c$, the samples can endure a considerable number of pulses without fracture. The latter can be explained by the change of the material properties connected with rebuilding the structure under the action of irradiation.[3,15,19] Fracture thresholds of thin samples do not depend, in fact, on the average electron energy E_e when energies are in the interval of 0.1–15 MeV, pulse durations τ equal 1–10 ns, and sample temperatures, 80–500 K. For irradiation at considerably smaller energies and densities fracture thresholds depend substantially on temperature.[8]

Experiments on the fracture of glass[19,23] evidence that the mechanical strength of glass fluctuates within wide limits, but the irradiation strength of glass is evaluated with great precision.

In anisotropic crystals, several sharply expressed fracture thresholds accord to the different directions of fracture; the typical histogram of distribution has two maxima[12] (see Fig. 3). The maxima are caused by the

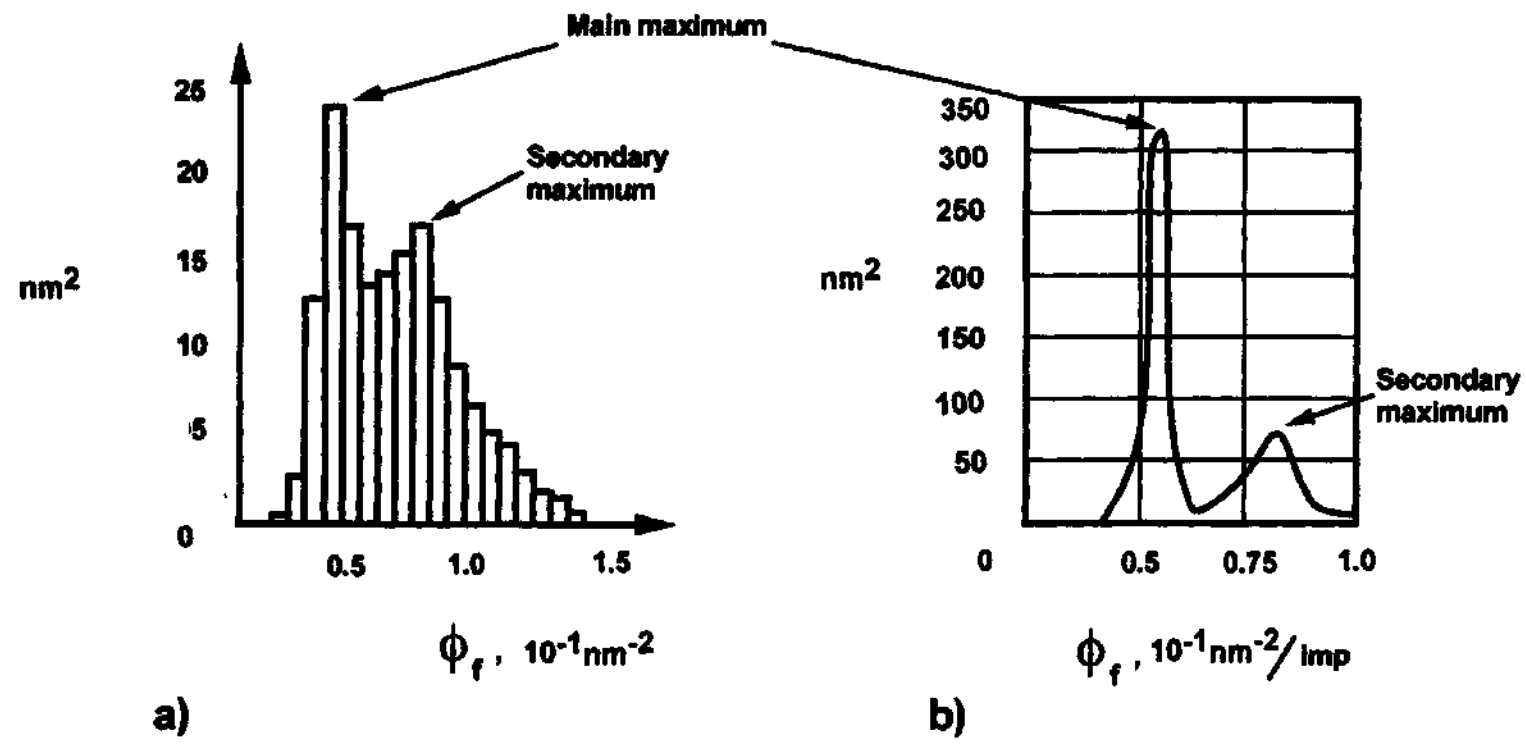

FIG. 3. Typical histograms of fracture threshold irradiation power rate for thin KCl specimens: (a) irradiation ensuring the fracture; (b) irradiation of individual impulse.

possible development of the splitting crack on different cleavage planes under similar conditions of irradiation. Fracture thresholds of all solids, while fracturing thin samples, do not depend on the macrodefects of the samples, and while fracturing dielectrics, splitting of the sample takes place in the undisturbed part despite the presence of microcracks or even previously created cracks.[21,35,39] (In some materials, splitting cracks can also grow from macrodefects.)

The microdefects of materials with a dislocation density of 10^6–10^{12} mm^{-3} exercise only weak influence on their irradiation strength. Preliminary irradiation and the so-called radiation hardening change irradiation thresholds of fracture insignificantly[22,28] despite the fact that the hardening increases dislocation density 10^3–10^4 times, with considerable increase of mechanical strength. Some data on the influence of preliminary irradiation on the fracture threshold of KCl crystals for plates with a thickness of $h_s = 300$ μm are shown in Table II. It should be mentioned that for preliminary hardening, the greatest effect is achieved by irradiation with light charged particles (electrons), while the slightest effect with slow neutrons; however, the fracture thresholds of "defectless" whisker crystals can drop several times (see Table I).

Increasing the sample thickness does not change the general character of fracture; it remains brittle, and there is a threshold irradiation energy; however, other factors, unnoticed before, begin to influence fracture properties. In addition to the main cracks splitting the sample, one can observe splitting out, swelling, and loosening of the surface on both sides of the sample.[15,27] Some materials carry traces of blast radiolysis: gas bubbles and surface erosion.[2] The density of the beam required for fracture Φ_f grows as the sample thickness increases; dependence of Φ_f on h_s for a single pulse is presented[12] in Fig. 4. Fracture of thick samples is influenced by already existing defects. With intermediate beam density, $\Phi_c < \Phi < \Phi_f$, a crack appears in the specimen, but it does not propagate through; cyclic irradiation results in further propagation of the crack and fracture. With subcritical density $\Phi < \Phi_c$ after several cycles of irradiation of thick samples, one can observe sub-

TABLE II. Fracture threshold of KCl crystals in terms of the preliminary irradiation power.

Type of preliminary irradiation	Energy of particles (MeV)	Total irradiation energy (J/nm^2)	Fracture threshold power rate of irradiation (W/nm^2)
No preliminary irradiation	···	0	0.08
Protons	6	3	0.096
Thermal neutrons	<1	100	0.083
	<1	1000	0.087
High-speed neutrons	>1	100	0.091
	>1	1000	0.095
Electrons	2	10	0.097

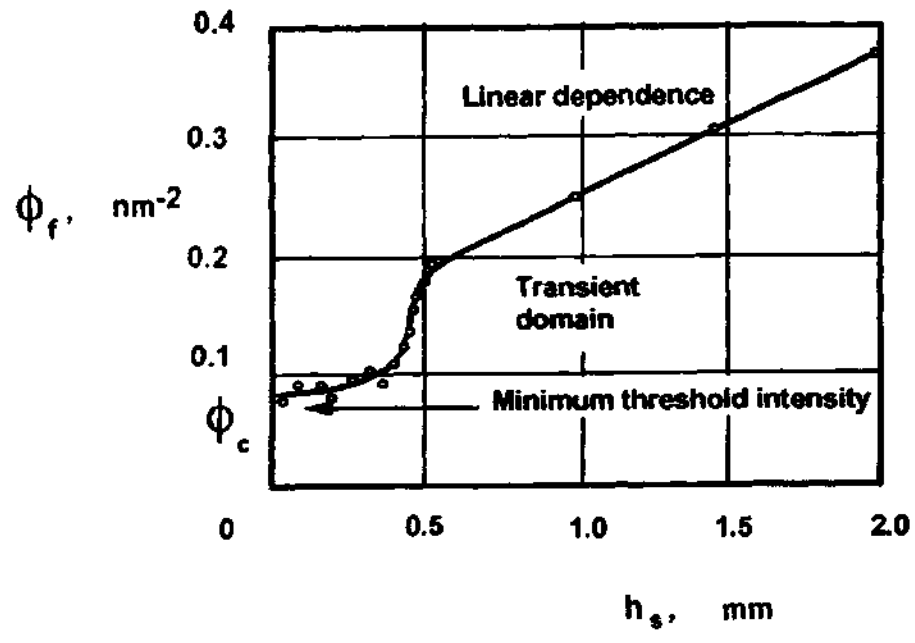

FIG. 4. Diagram of the fracturing beam density Φ_f vs sample thickness h_s for a single pulse.

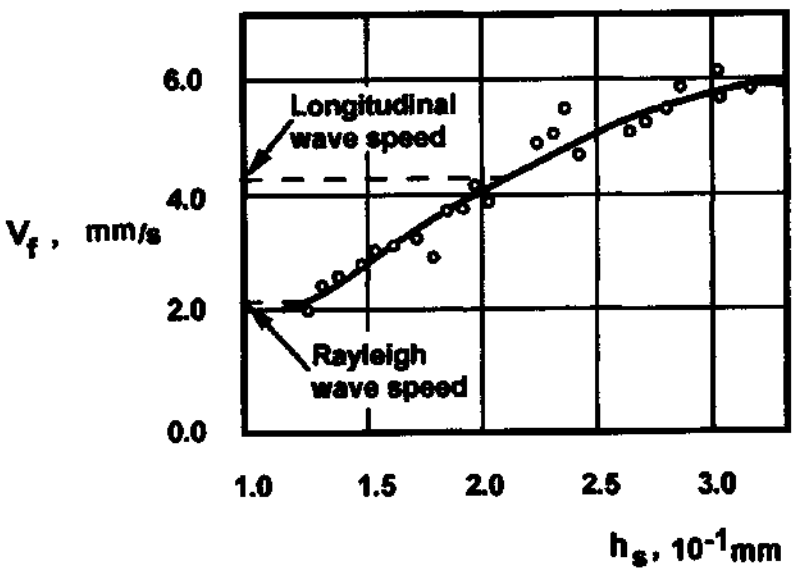

FIG. 5. Dependence of fracture velocity v_f for KCl and NaCl vs thickness of specimen h_s.

critical growth of already existing cracks or microcracks of the material, i.e., a shift of the fracture threshold occurs under prolonged exposure, and the fracture of samples is accompanied by the appearance of a great number of cracks.[2]

The speed of crack growth in the material under normal conditions is determined by the rate of energy fed to the end of the moving crack. Under usual mechanical loading in isotropic elastic media, the speed of crack growth V_c is limited by the value c_* at which branching takes place, $c_*=c_s/2$, where c_s is the velocity of shear waves in the medium. If the rectilinear direction of crack growth is predetermined, e.g., by anisotropy of the material, the maximum speed of crack growth under the influence of external forces will be[34,42] the speed of Rayleigh waves c_R. If the growth of the fracturing crack begins inside the specimen, the speed of fracture $V_f=h_s/\tau_f$, where h_s is the sample thickness and τ_f is the time to sample fracture, will exceed the speed of crack growth in one direction V_c. In the limiting case of splitting from the center of the sample, the speed of fracture can reach the value of $2V_c$. Thus, the maximum value of the fracture speed for an isotropic plate under normal conditions is $2c_*$, and for anisotropic, $2c_R$.

Many authors[11,12,15,19,26] observed high speeds of fracture considerably exceeding both the speed of Rayleigh waves and that of transverse and longitudinal elastic waves while fracturing solids by powerful relativistic electron beams. Although exact experimental measurements of fracture speeds are very scarce, the data are reliable and significant: Average fracture speeds mentioned in these articles exceeded the maximum speed of brittle fracture $2c_R$. For instance, while fracturing KCl and NaCl crystals, the average fracture speed V_f reached values of more than $3c_R$ (see Fig. 5). In this case, the speed of longitudinal elastic waves is: $c_p=4500$, $c_s=2.4$, $c_R=2.3$, and $c_*=1.5$ K m/s. These data show that the fracture of solids with powerful electron beams differs considerably from usual brittle fracture and other types of quasibrittle, tough, or ductile fracture.

It should be noted that the methods of measuring fracture speeds by secondary current pulse give only a crude estimate of the lower bound of crack growth speed for the following reasons.[12] First, the speed of fracture can exceed the average value to a great extent. Second, the fracture process lasts considerably longer ($\sim 10^{-7}$ s) than the irradiation pulse that causes it ($\sim 10^{-8}$ s); thus, the average fracture speed can result from considerably different speeds of crack growth at different stages of propagation. Third, the exact place of crack emergence is not known, and even the average crack speed V_c determined from the data on fracture speed V_f can differ within the interval $V_f/2<V_c<V_f$. Hence, the speed of crack growth can exceed averaged experimental values to a very great extent.

It is worth noting that in the case of optical fracture caused by laser rays, the speed of crack growth can exceed the speed of elastic waves several times.[43–45] Even crack speeds of the order of $100c_s$ were registered.[45] Probably some resemblance must exist between the mechanisms of electron and optical fracture.

Another specific feature of fracture by powerful electron irradiation is connected with a small number of the cracks fracturing the sample. As already mentioned above, even for beam parameters that considerably exceed threshold values, usually only one crack appears. The number of splitting cracks increase only to two or three for a beam density two to three orders of magnitude higher than the threshold density.

All of the preceding phenomena connected with the fracture of solids by powerful relativistic electron beams manifest themselves very clearly for dielectrics (for alkali-haloid crystals, in particular). We should stress the unexpected peculiarity of the fracture of dielectrics: Macrodefects in the samples do not affect fracture. Even with the weakening of samples by means of cracks made beforehand, irradiation fracture takes place in some virgin region of the sample. Apparently, the mechanism of the fracture of dielectrics by relativistic electron beams of high intensity is connected with the continuity of the medium.

Other effects of the irradiation of solids by high-energy electron beams are not connected directly with the fracture of materials. However, these are observed only while irradiating materials by relativistic electron beams and they do not depend upon the temperature and purity of the crystals.

The very large increase in electric conductivity of dielectrics with electron irradiation is not a threshold phenomenon and is connected only with electron beams; it is not observed with neutron, proton, or photon irradiation.[13,21,46] The electrical conductivity of the material σ can increase considerably, by three to four orders, even if irradiation intensity Φ is smaller than the threshold intensity Φ_c. Near the fracture threshold, σ reaches values of the order of 10 Ω^{-1} m^{-1}, which is 10^{13}–10^{15} times larger than the initial value (e.g., for a threshold beam density, the resistance of the KCl sample corresponds to the resistance of a similar metal sample under usual conditions). The dependence of the pulse electrical conductivity σ on the density of electron irradiation for the KBr samples is shown[23] in Fig. 6. Relaxation time for the intensive component of conductivity is very short. In the same work, it is noted that even for a high-speed oscilloscope with a resolving power of 10^{-1} ns it is impossible to determine the shape

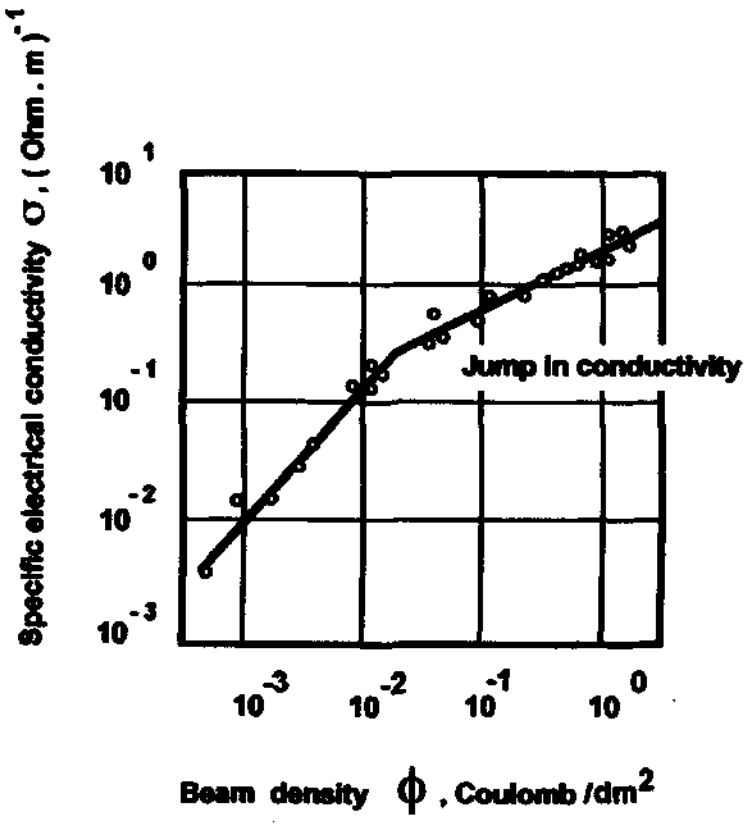

FIG. 6. Dependence of the specific electrical conductivity σ on the electron beam density Φ for the KBr sample.

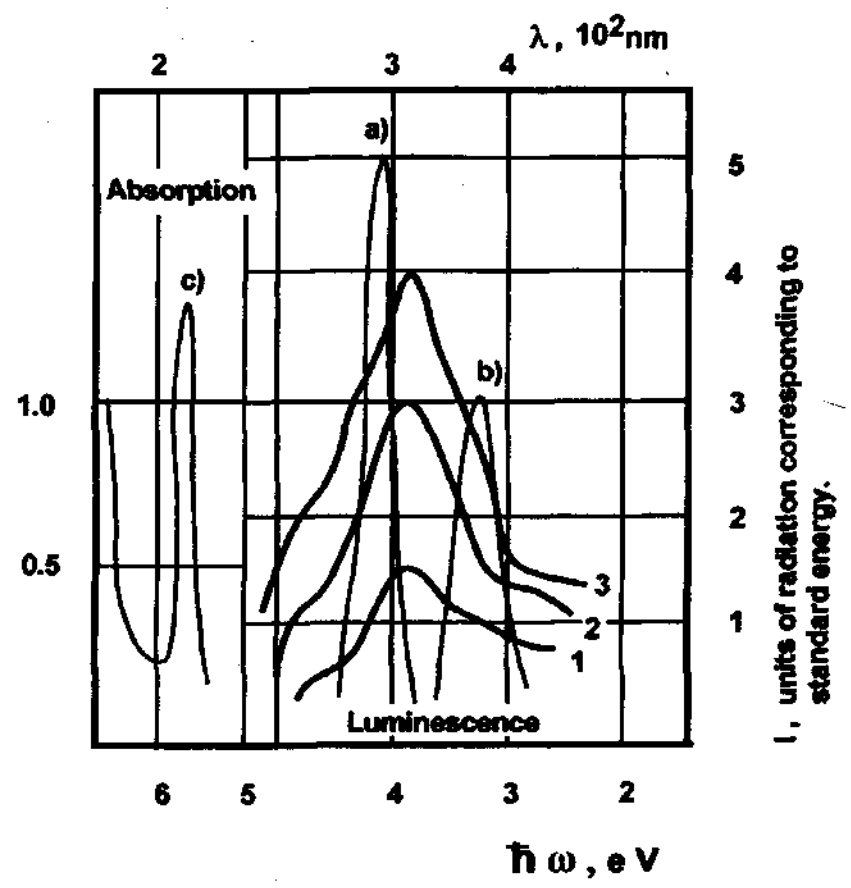

FIG. 7. Spectra of light pulse radiation of KI: (1) for $\Phi=25$; (2) for $\Phi=11$; (3) for $\Phi=24$; Coulomb/hm^2. The thin lines are (a) standard singlet; (b) triplet luminescence; and (c) fundamental absorption spectrum.

of the current pulse signal; the authors evaluated the time of existence of the effect with values of the order of 10^{-12} s. (This value is comparable to the time, $1–10^{-1}$ ps, the electromagnetic disturbance passes through such a sample.) As external voltage increases, the pulse electrical conductivity grows weakly; for a voltage of -600 to $+600$ V (corresponding to fields of 10 MV/m with the intensity of the internal field of the solid being[31] of the order of 1–100 GV/m), the increase of σ does not exceed 30%. The immense increase in the conductivity of dielectrics in the interval 80–400 K does not depend on temperature. This fact, as well as the ultrashort time of relaxation of the effect, proves that charge carriers are fast electrons. The kinetic energy of these carriers must considerably exceed the energy of the thermal electrons, which is about 0.1 eV.

The typical dependence of σ on flux Φ (see Fig. 6) shows a sharp change of the rate of increase with the irradiation density ($\Phi\sim10^{-4}$ C/m^2, where C/m$^2=6.2\times10^{20}$ electrons/m^2 in the case of an electron beam). Beginning from such values of Φ, of the order of 10^{-4} C/m^2 for dielectrics, one can observe the characteristic glow with a subnanosecond time de-excitation, considerably shorter than in the case of fundamental singlet luminescence of excitons;[19,31] the entire irradiated sample glows evenly. It is worth noting that the purity of the crystals has a very weak effect on glowing, and the glow intensity within the interval of 80–500 K does not depend on temperature. Characteristic features of the glow are as follows (see Fig. 7): (a) The half-width of the radiation spectrum is 1.5–2 eV; (b) radiation occurs in the ultraviolet and visible spectral region with frequency threshold $\hbar\omega=5$ eV (corresponding to a wavelength of the order of 2500 Å); (c) for a number of crystals, for KI in particular, the large wavelength tail of radiation obeys the power law of $-3/2$; (d) some structure appears that superimposes a wide band of spectrum characteristics.

Figure 8 shows[19,23] the dependence of glow intensity of KI crystals on Φ for a subnanosecond glow at 80 K and exciton glow at 400 K. Note that the glow intensity grows as Φ increases, but a section of the curve after $\Phi=10^{-3}$ C/m^2 can probably indicate the presence of some different glow mechanisms.

From a practical point of view, the most interesting prospect is the application of high-voltage accelerators for fracturing rocks. Here are the most important conclusions deduced from the first experimental data[1,25,47] concerning the fracture of a number of rocks: (a) The fracture is brittle and results in the formation of a few large fragments and many tiny particles whose total volume is very small; (b) a low-power intensity of fracture, of the order of 10^8 J/m^3, is characteristic of rocks with different mechanical strengths—up to the strongest of them, such as basalts, gneisses, etc.

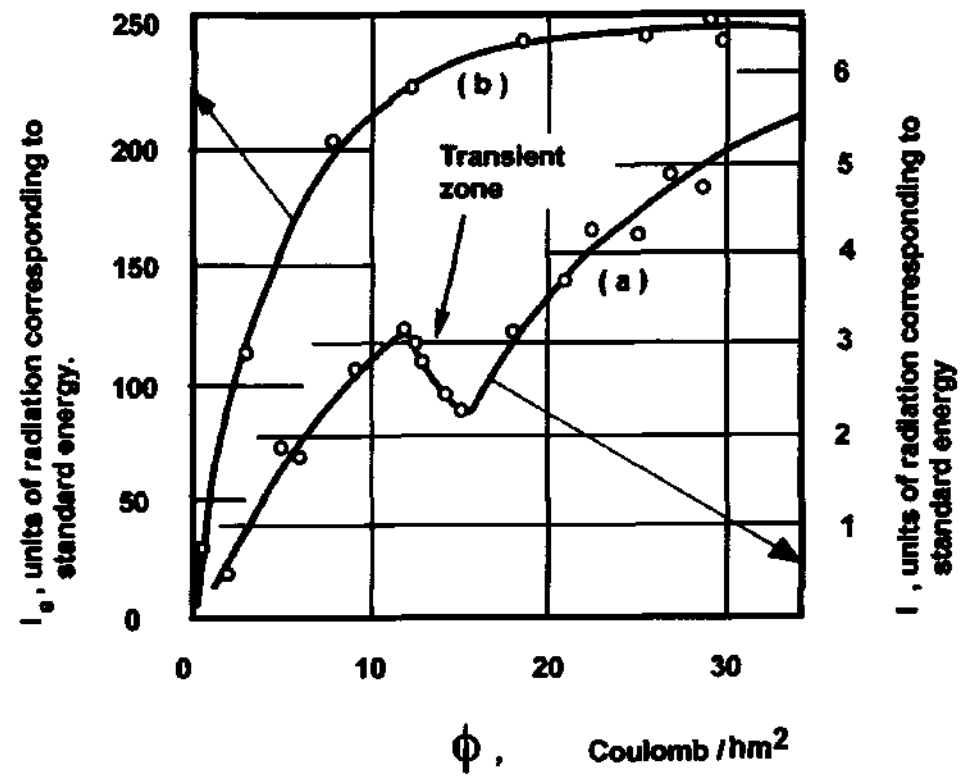

FIG. 8. Dependence of glow intensity in (a) subnanosecond and (b) exciton range on irradiation beam density Φ for KI crystal.

C. Models and problems of the theory of the electron fracture mode

Experimental data show that electron fracture exceeds the limits of conventional notions of viscous, ductile, brittle, or mixed fracture of solids.[34,47–50] At the same time, this fracture proceeds in a "brittle" way, i.e., at the expense of one or two considerable cracks propagating in a solid, which indicates the mechanical nature of splitting the material. However, as one can judge from the peculiarities of the fracture of disturbed samples and supersonic crack growth registered in the experiments, such splitting (or cutting) of a solid cannot be produced by means of energy flow to the end of the crack through the nucleons of the solid. It is natural to presume the existence of a physical mechanism which, beginning from a certain critical value of the beam density of relativistic electrons (or the absorbed energy), causes the formation of macroscopic electron clusters in a solid. The contradiction between the mechanical character of brittle cleavage and its peculiarities is then removed entirely. The electron clusters of solid plasma become the mechanical object whose high-speed progress causes material cleavage. (The mean-square-law speed of fluctuations in solid plasma reaches values[12,51] of the order of 1 Mm/s, which considerably exceeds the speed of elastic waves in a solid.) Furthermore, supersonic progress of the plasma clusters, like a knife or a wedge cutting a body, will be accompanied by shock waves in a solid. The existence of shock waves in a material fractured by irradiation with powerful electron beams was observed in many works.[4,7,32,52,53]

This explanation (and the corresponding fracture pattern) is called electron fracture mode (EFM) in the succeeding text. The problems of defining the physical mechanism causing the formation of electron clusters in a solid are also to be studied, as well as the problem of determining the laws of the motion of clusters cutting the body. To solve these problems, the present article considers the interaction taking place in the powerful relativistic electron beam in a continuum medium, in which the effect of the self-packing of particles in the beam is discovered. The problem of cutting a solid by a "knife" moving with supersonic speeds is utilized to find the length of a final crack.

This approach can be considered only as a first approximation to the reality. The full picture of these phenomena must also take into account the effects of the usual types of viscous, brittle, or ductile fracture, and effects of excitation in the electron subsystem of a solid. Some authors reported the existence of several different mechanisms for fracturing solids by means of powerful relativistic electron beams, including electrical breakdown,[2] the mechanical effect of the electron beam,[12] and the thermomechanical effect.[26] There is some mention of the relativistic effects of the excitation of the bound electrons of the material.[23] Notice that it was proved experimentally that the above three mechanisms barely influence the observed fracture.[15,16,18] Different explanations of electron fracture, such as thermal-shock fracture,[1,7] accumulation of internal microvoltages,[2,54,55] and the waves of elastic and thermal stresses,[20,40] do not explain the main peculiarities of EFM by the electron irradiation.[35,56] The suppositions about the leading role of solid-body plasma, which can be turned into a condensed state in the process of fracture,[12,39,53] may be interesting for the mechanism of plasma "wedge" or "knife" initiation and some effects of the initial stage of the process.

The noncontinuum approach to the description of supersonic fracture was suggested by Sanders[57] using an ideal lattice in which the crack growth rate is determined by the rate of energy input. Fracture on the atomic level within the framework of a one-dimensional model of a limited chain, analogous to Sanders's model, was also considered.[55]

II. FORMULATION OF PROBLEMS OF THE THEORY OF ELECTRON FRACTURE MODE (EFM)

A. Interactions in relativistic electron beams

The electron beams used for the fracture irradiation of solids are relativistic and, moreover, the particle velocities surpass the phase speed of electromagnetic waves (the speed of light) in the material medium, for example, in dielectrics. The existence of these electrons was discovered by Cherenkov[58–60] and Vavilov.[61] The theoretical description of the motion of an individual superluminal electron and the explanation of the irradiation that arose in the case of this motion were given by Tamm and Frank[62] and Tamm.[63]

The phenomenon of the motion of Cherenkov's superluminal electrons and the Cherenkov–Vavilov irradiation are analogous to the formation of shock waves for electron motion with velocities faster than elastic-wave speeds in a continuum.[63] The electromagnetic field of a superluminal electron differs principally from the field of a stationary charge as follows: In the charge wake inside the Mach cone only, the components of the electromagnetic field change sign when the charge velocity passes the phase velocity of light. This difference completely changes the nature of the interaction for electron beams moving with superluminal velocities.

The energy dissipation of an electron (and its deceleration in a medium) depends on the interaction of the electron's field with external electromagnetic fields existing in this media (the bremsstrahlung and ionization), on the wave losses on the Mach cone fronts (the Vavilov–Cherenkov irradiation), and on the collective interaction with the fields of other beam electrons. The interactions of the first and second kinds are approximately equal for all beam particles at great speed, and these interactions exert negligible influence on the mutual spatial distribution of electrons in the beam. Therefore, this distribution is determined mainly by their collective interaction. Therefore, only the collective interaction of electrons is studied below.

The electromagnetic interaction of two or more charges moving with superluminal velocities in a continuum medium was studied by Borzykh and Cherepanov.[64] The interaction law of two charges is necessary for investigation of collective interactions. The technique based on the invariant Γ integrals[65–68] of the mechanics of an elec-

tromagnetic deformable continuum reveals the interaction law of two charges and allows study of collective interactions.

The collective interactions are considered here on the assumption that all particles have the same constant velocities. This statement of the problem is correct for the times much smaller than the time of existence of superluminal electron beams in a medium, and it permits the simple estimations of the process parameters. We note, too, that mutual distribution and collective interaction are considered in the proper coordinate frame moving with electrons, and the relativistic effects of the shortening of the length and time are significant for these systems.[69–73]

For the study of collective interactions, we use the known solution[74] of the Maxwell equations for the proper field of a charge moving with constant velocity V, which is more than the phase speed of light in medium a and less than the speed of light in vacuum c. The asymptotic representation of the steady-state field of a superluminal negative charge e moving along the x_3 axis in the proper space-time coordinates x_1, x_2, x_3, t according to the Lorentz transformations is

$$E_i=\frac{eM^4x_i}{2\pi\epsilon'(x_3^2-M^2r^2)^{3/2}} \quad (i=1,2),$$

$$E_3=\frac{-eM^2x_3}{2\pi\epsilon'(x_3^2-M^2r^2)^{3/2}}, \qquad (2.1.1)$$

$$B_1=Ax_2, \quad B_2=-Ax_1,$$

where

$$A=\frac{\mu^1eVM^2(1-a^2/c^2)}{2\pi(1-V^2/c^2)(x_3^2-M^2r^2)^{3/2}}, \quad B_3=0. \qquad (2.1.2)$$

Here,

$$M^2=\frac{(V^2/a^2)-1}{1-(V^2/c^2)}=\frac{\mu\epsilon V^2-c^2}{c^2-V^2}>0,$$

$$a=\frac{c}{\sqrt{\mu\epsilon'}}, \quad \mu'=\mu\mu_0, \quad \epsilon'=\epsilon\epsilon_0,$$

where E_1, E_2, E_3, B_1, B_2, and B_3 are the electromagnetic field components of the $x_1x_2x_3$ system, a is the phase speed of light in the medium, and M is the relativistic Mach number (ϵ_0 and μ_0 are the absolute dielectric and magnetic constants of the medium, respectively). The field described by the solutions, Eqs. (2.1.1) and (2.1.2), is defined inside the Mach cone, i.e., in the region $x_3^2>M^2r^2$, $x_3<0$; outside this cone, the field of the electron vanishes.

B. Mechanical model of the supersonic cutting of solids

The phenomenon of the supersonic crack can be explained by the existence of some macroscopic objects moving in solids with velocities faster than those of sound.

In the following, we assume that there are some conditions of plasma cluster formation that cut solids like a "wedge" or a "blade." These conditions exist at the beginning of fracture by some critical intensity of irradiation. This idea is analogous to that of the mechanism of fracture induced by a plasma jet for high-power pulsed-laser irradiation.[43–45] The velocity of plasma jet propagation is faster than elastic wave speeds, too. The large supersonic velocities of the plasma blade cause the same persistent pressure of the blade on the surface of the propagating cracks at their tips. The motion of a finite-length plasma blade can form a narrow canal of fracture or a fracture plane. In the above case, the maximum probability of the crack orientation would be along a minimum-strength plane, such as the cleavage planes of a crystal. It is obvious that the irreversible deformations would not have time to develop on the sides of a resulting crack in the case of supersonic cutting.

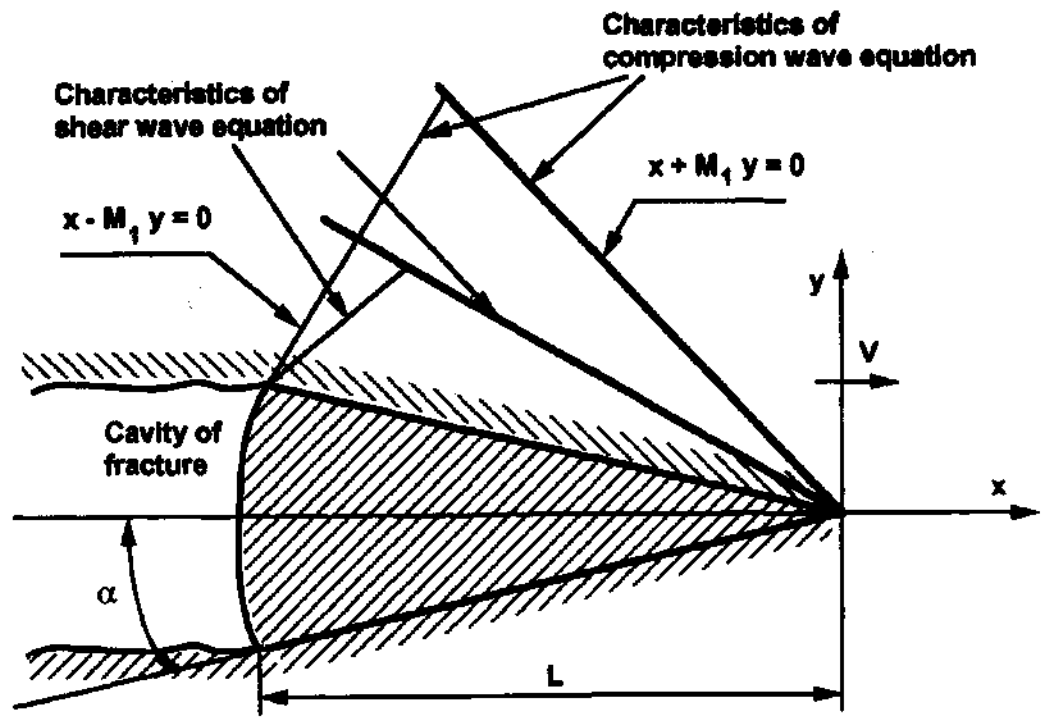

FIG. 9. A thin wedge moving in an elastic solid with a supersonic velocity (M is the Mach number).

We note, too, the following known dynamic problem of elasticity: the supersonic motion of a point load on the boundary of a half-plane.[75] The solution to this problem is analogous to that of a similar acoustic problem,[76] complicated by the fact that in elasticity there is the system of two wave equations and two wave fronts. The supersonic motion of a finite plasma blade is analogous to the flow past a thin wing in gas dynamics.

According to these introductory notes, the problem of supersonic cutting is solved below within the framework of the model assumptions about an absolutely rigid wedge and an ideally elastic material. Electron fracture is a complicated phenomenon, and detailed information on the properties of solid plasma clusters and their behavior in a material is lacking. Therefore, some simplifications are needed for a preliminary description of the electron fracture mode and will permit the eventual study of the phenomenon later.

Suppose that a thin, rigid wedge of length l moves in an infinite elastic space with supersonic velocity V. The wedge angle is equal to 2α (see Fig. 9), and the direction of movement is the x axis. The two-dimensional problem is assumed to be symmetric relative to the x axis; the z coordinate directed along the wedge edge is nonessential. The

surface of the resulting cavity outside the contact zone is a free boundary. The law of wedge motion with the initial supersonic velocity V_0 must be found. The boundary condition is

$$V_n=0 \quad \text{on } \Sigma_w, \tag{2.2.1}$$

where V_n is the normal velocity at the contact surface Σ_w. The condition of contact friction is

$$\sigma_{tn}=F(\sigma_n,V_t), \tag{2.2.2}$$

where the directions of the tangent and the normal of the contact surface Σ_w are, accordingly, t and n; the normal and shear stresses are σ_n and σ_{tn}; and the normal and tangent components of the material velocities are V_n and V_t. The function F is a known frictional characteristic found from an experiment, or from the model ideas; for example, we will assume $\sigma_{tn}=f\sigma_n$, where f is the Coulomb friction coefficient.

The statement of the problem is closed using the conditions of mass and momentum conservation on two Mach fronts, where velocities and stresses are discontinuous.

C. Invariant gamma integrals of dynamic problems of mechanics of a deformable, electromagnetic continuum described by hyperbolic differential equations

The state of electromagnetic deformable matter can be characterized by field vectors **E**, **B**, **D**, and **H**, displacement vector **u**, velocity vector **v**, stress tensor σ_{ij}, and a certain strain tensor ϵ_{ij}. The following equations hold:

Maxwell's equations:

$$\gamma_{ijk}\mathbf{E}_{j,k}+\frac{\partial \mathbf{B}_i}{\partial t}=0, \quad \gamma_{ijk}\mathbf{H}_{j,k}-\frac{\partial \mathbf{D}_i}{\partial t}=J_i,$$
$$\mathbf{D}_{i,i}=\delta, \quad \mathbf{B}_{i,i}=0, \quad J_{i,i}+\frac{\partial \delta}{\partial t}=0; \tag{2.3.1}$$

Newton's equations:

$$\sigma_{ij,j}=\frac{d(\rho v_i)}{dt}-\rho F_i. \tag{2.3.2}$$

The local law of the conservation of energy is

$$\dot{U}=q_{i,i}+E_i\dot{D}_i+H_i\dot{B}_i+\sigma_{ij}\dot{\epsilon}_{ij}. \tag{2.3.3}$$

The kinematic conditions for any finite strains are

$$2\dot{\epsilon}_{ij}=v_{i,j}+v_{j,i}, \quad v_i=\dot{u}_i. \tag{2.3.4}$$

Here, J is the current density vector; δ is the charge density; ρ is the density of the matter; x_1,x_2,x_3 are the rectangular Cartesian coordinates; t is time; $\mathbf{u}_1$, $\mathbf{u}_2$, and $\mathbf{u}_3$ are displacement components; **q** is the vector of the net heat flux; $\dot{U}$ is the rate of change of the internal energy of a matter per unit volume; the dot over a letter refers to the total derivative with respect to time; and $\gamma_{123}=\gamma_{231}=\gamma_{312}=1$, $\gamma_{132}=\gamma_{321}=\gamma_{213}=-1$, all other γ_{ijk} being equal to 0. The strains of the medium are arbitrary ($\dot{\epsilon}_{ij}$ is the strain rate tensor).

All functions in these equations are assumed continuously differentiable the necessary number of times throughout the investigated region, with the exception of singular points, singular lines, and singular surfaces, at which these equations make no sense.

Surface invariant Γ integrals of the first kind[66,67] are

$$\Gamma_k=\int_\Sigma [(\ni+F+\tfrac{1}{2}\rho\dot{u}_i\dot{u}_i)n_k+(\mathbf{D}_i\mathbf{E}_k+\mathbf{B}_i\mathbf{H}_k-\sigma_{ij}u_{j,k}-q_{i,k})n_i]d\Sigma \quad (i,j,k=1,2,3). \tag{2.3.5}$$

Here Σ is a surface in the coordinate system, x_1,x_2,x_3; $\ni$ and F are the following potentials:

$$\ni=U-\mathbf{E}_i\mathbf{D}_i-\mathbf{H}_i\mathbf{B}_i,$$
$$F=-\int\left(\frac{\partial P_i}{\partial t}+\rho\mathbf{E}_i+\gamma_{ijk}J_i\mathbf{B}_k\right)dx_i, \tag{2.3.6}$$
$$P_i=\gamma_{ijk}\mathbf{B}_j\mathbf{D}_k.$$

In the case of the physical field, which is steady with respect to Σ, the following theorems were proven.[66,67]

Theorem 2.3.1: Γ integrals do not change their value along any closed surface Σ encompassing a singular point, singular line, or singular surface. Surface Σ can be arbitrarily deformed without changing the value of the Γ integrals, if in the deformation process surface Σ does not intersect a singular point, a singular line, or a singular surface.

Theorem 2.3.2: If an open surface Σ is limited by a three-dimensional contour L, the Γ integrals do not change their value with any deformation of the surface Σ, so long as (a) contour L is fixed, and (b) surface Σ does not intersect a singular point, a singular line, or a singular surface in the process of deformation.

In a Cartesian coordinate system x_i' moving at constant velocity **V** coinciding with that of beam electrons, the Γ integrals are found from Eq. (2.3.5) by the transformations $x_i \to x_i'$, $\dot{u}_i \to \dot{u}_i' - V_i$. Theorems 2.3.1 and 2.3.2 are true in the x_i' coordinates for moving surface Σ fixed with beam electrons in the case of thermodynamically reversible media, or for any media by steady processes when $k=1$.

Supersonic or superluminal motions of singularities: The theory of the motion of singularities[65–67] is detailed here for the case of velocities faster than the speed of propagation of sonic, luminal, and other processes.

To be specific, consider a singular point O_s, moving with a superluminal or supersonic velocity. This motion forms a moving, singular surface Σ_s (or a family of singular surfaces for different wave processes), joined with the singular point O_s. If the motion of O_s is a locally steady process, surface Σ_s is the conic surface $x_3^2 = M_*^2 r^2$, $x_3<0$, near the point O_s, where the x_3 axis is collinear with the velocity vector **V**; M_* is the Mach number of the relative wave process with characteristic speed, c_*; and M_*^2 and r^2 are

$$M_*^2=V^2/c_*^2-1>0 \quad \text{and} \quad r^2=x_1^2+x_2^2,$$

where x_1, x_2, and x_3 are moving coordinates. By considering the motion of a singularity from time $t=0$ of its creation at some inner point of a continuum, we see that in time t a domain of the field of singularity O_s will have the

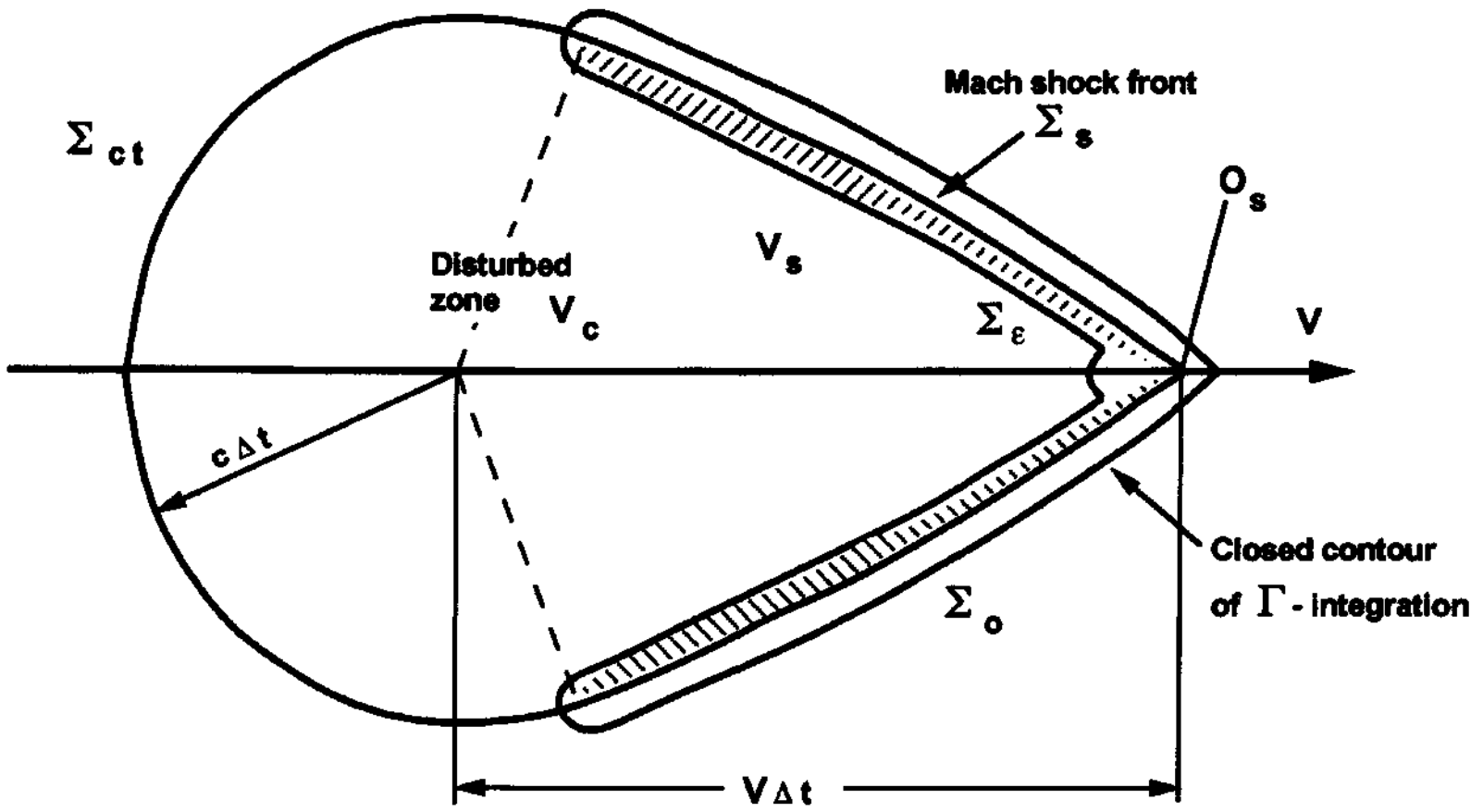

FIG. 10. The perturbation zone axial cross section of a moving point singularity.

form shown in Fig. 10; outside this domain V_c the field is equal to zero. The surface that bounds V_c consists of two parts, such that the singular surface Σ_s is the surface of an axisymmetrical, curvilinear Mach cone, and Σ_{ct} on Σ_s is a shock wave front, with the components of velocities, stresses, and other field parameters being discontinuous; Σ_{ct} is the rear wave front of disturbances arising at $t=0$.

Let us surround O_s and Σ_s, which are a singular point and a singular surface, with any closed surface Σ_0 in the neighborhood of Σ_s, such as shown in Fig. 10; single out the separate region Σ_ϵ on Σ_0. The Σ_ϵ is a part of the small sphere with radius ϵ that tends to zero (on the outward part of Σ_0, this difference is nonessential since the field of singularity is absent outside V_c). For simplicity, the field is assumed to be continuous along Σ_{ct}. Let us consider the Γ integrals over Σ_0, which are equal physically to an energy flux flowing into Σ_0. All the integrand functions in Eq. (2.3.5) are assumed differentiable in V_c, except Σ_s and O_s on Σ_s. On Σ_s some functions may be infinite.

The energy dissipation at O_s and Σ_s is equal to

$$dA=\Gamma_i\,dx_i, \tag{2.3.7}$$

when O_s advances on $dx_i=\mathbf{V}_t\,dt$ during the time, dt. Here, $\mathbf{V}_1$, $\mathbf{V}_2$, and $\mathbf{V}_3$ are velocity components of the singular point, and A is the field energy of the system.[65–67]

Hence, we have

$$\Gamma_i=\frac{\partial A}{\partial x_i}, \tag{2.3.8}$$

where Γ_i is the specific energy dissipation at O_s and Σ_s per unit length of advance of O_s along the x_i axis. The energy dissipation rate is equal to

$$\dot{A}=\Gamma_i V_i. \tag{2.3.9}$$

The invariant properties of Γ with respect to the integration surface greatly simplify the calculations.

For the supersonic or superluminal singularities under consideration, the singularity O_s is the source of energy flowing down the singular surface Σ_s, which is the sink of energy. Some examples of this dissipation include the shock wave in gas dynamics or the Cherenkov–Vavilov radiation of superluminal electrons in dielectrics.

In the case under study, the singularity is an electron; hence, Γ_1, Γ_2, and Γ_3 are equal to corresponding components of the force applied to the electron as a drag.

In the general case of a nonzero external field outside V_c, the Γ integral over Σ_ϵ (which is denoted by $\Gamma_{\epsilon i}$) is the following sum:

$$\dot{A}_0+\dot{A}_s=\Gamma_{\epsilon i}V_i. \tag{2.3.10}$$

Here $\dot{A}_0$ and $\dot{A}_s$ are dissipation rates in external and internal fields obtained by integration over the outer and inner sides of Σ_0, respectively.

In the special case of the steady motion of a singularity that corresponds to the infinite time of the motion of the singularity, the disturbed zone is the infinite cone (or some cones of different wave processes), as shown in Fig. 11. The complete integration surface Σ_0 consists of Σ_0^+ and Σ_0^-, which are the inner and outer sides of Σ_0. The surface Σ_0^+ is inside the disturbed zone and Σ_0^- is outside it. If the limits of the Γ integrals over $\Sigma_0=\Sigma_0^++\Sigma_0^-$ for $t\to\infty$ exist, they provide the complete dissipation $\dot{A}_s$ and $\dot{A}_0$.

The sign of $\dot{A}_0$ can be positive or negative depending on the nature of an external field that can either absorb the energy of the point source or feed an internal field inside V_c. The sign of $\dot{A}_s$ is always positive because it corresponds to the dissipation of energy.

The value of Γ is defined as the result of calculating the Γ integral over Σ_ϵ when $\epsilon\to 0$, since the axis of the light cone coincides with the direction of motion of the electrons. In gas dynamics, Γ equals the wave drag experi-

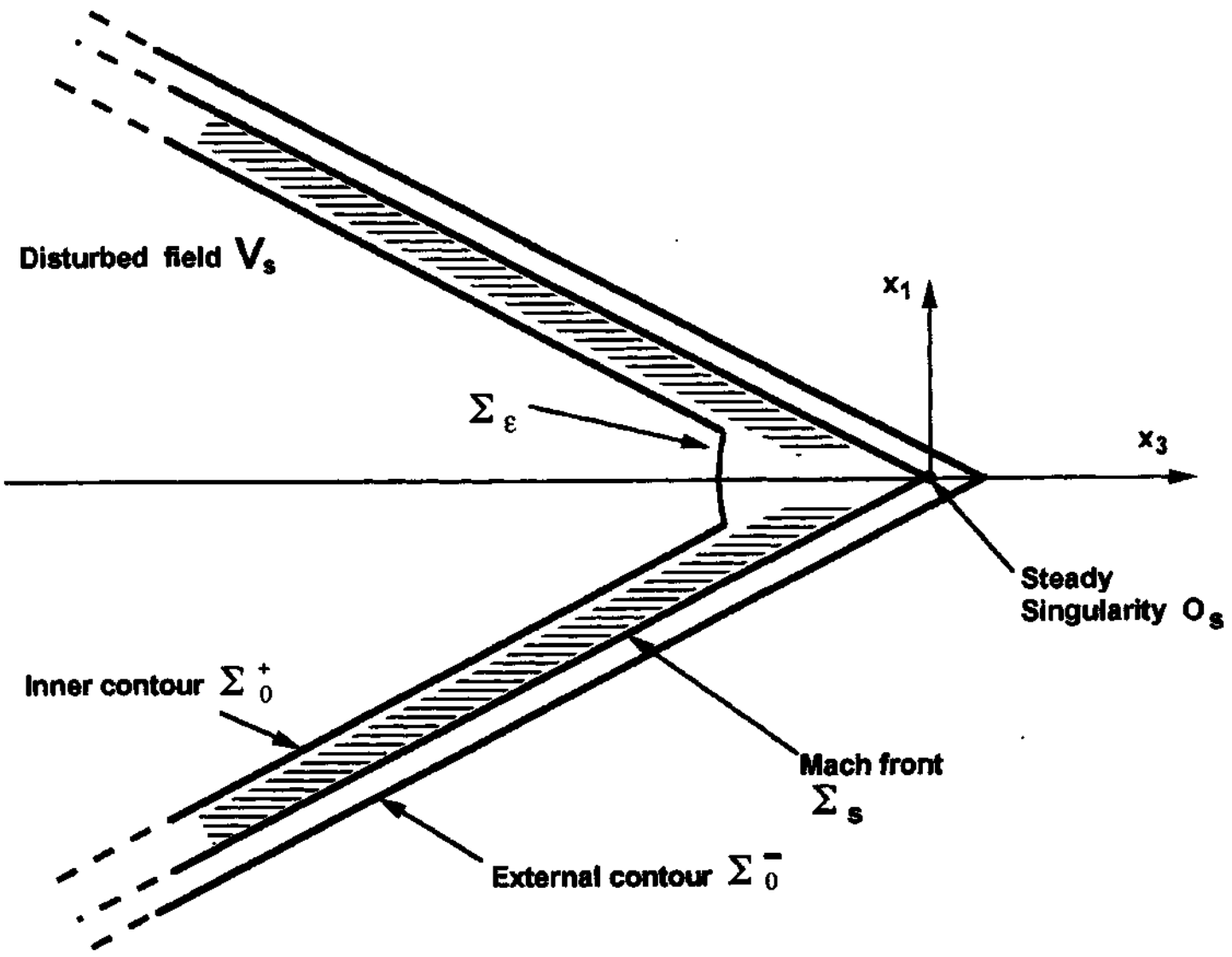

FIG. 11. Surface of integration near a point singularity.

enced by a moving body, and in electrodynamics, Γ is the decelerating radiation energy of Cherenkov–Vavilov.

In the problem under study, according to Eqs. (2.1.1) and (2.1.2), the field is steady state, not only in the vicinity of O_s, but also all over the disturbed domain V_c.

The problem is well posed if its solution provides a finite value of Γ; otherwise, the problem is ill posed. Well-posed problems permit determination of the physical characteristics of singularity; namely, a drag, a specific dissipation, etc. It should be noted that asymptotic forms of different kinds of moving singularities are different near the singular fronts, and improper Γ_ϵ integrals usually are divergent integrals.

In order to compute invariant integrals divergent at singularities, we apply an heuristic rule of Γ integration,[65–68] which requires taking into account only the finite part of the integration result. Furthermore, the integration surface in the neighborhood of a singularity should be symmetrical.

As to the problem under study, symmetry is achieved provided that the integration surface in the near neighborhood of an electron Σ_ϵ, is spherical (Figs. 10 and 11) or is an axisymmetrical, circular cross section of the Mach cone in the same neighborhood (see the following section).

Particular forms of invariant Γ integrals in different media used in the moving coordinate frame with respect to which physical field is steady are listed here:

(i) a compressible gas,[47,77]

$$\Gamma_i=\int_\Sigma (\rho \mathbf{v}_i \mathbf{v}_j/n_j+pn_i)d\Sigma \quad (i,j=1,2,3), \tag{2.3.11}$$

where p is pressure and $\mathbf{v}_i$ is a gas velocity component;

(ii) an electromagnetic field in a dielectric,[78]

$$\Gamma_i=\int_\Sigma [(\mathbf{D}_j\mathbf{E}_i+\mathbf{B}_i\mathbf{H}_j)n_j-\tfrac{1}{2}(\mathbf{D}_j\mathbf{E}_j+\mathbf{H}_j\mathbf{B}_j)n_i]d\Sigma, \tag{2.3.12}$$

(iii) a linear or nonlinear elastic medium,[65]

$$\Gamma_i=\int_\Sigma [(U+\tfrac{1}{2}\rho \mathbf{v}_k\mathbf{v}_k)n_i-\sigma_{kj}u_{k,i}n_j]d\Sigma. \tag{2.3.13}$$

In a static case, velocities equal zero ($\mathbf{v}_k=0$), and the latter equation provides an invariant J integral.[34]

III. SELF-COMPRESSION OF RELATIVISTIC ELECTRON BEAMS IN A MEDIUM

A. Individual electron with a superluminal velocity in a dielectric medium in the case of an external field

Let us consider the motion of an individual electron with negative charge e having a constant superluminal velocity V in a homogeneous, external electromagnetic field $\mathbf{E}_0=\{E_{oj}\}$ and $\mathbf{B}_0=0$ in a dielectric. The proper singular field $\mathbf{E}_s$ and $\mathbf{B}_s$ of this electron is determined by Eqs. (2.1.1) and (2.1.2). According to the principle of superposition based on the linearity of Maxwell's equations, the complete field near the individual electron is

$$\mathbf{E}=\mathbf{E}_s+\mathbf{E}_0, \quad \mathbf{B}=\mathbf{B}_s+\mathbf{B}_0. \tag{3.1.1}$$

The proper dissipation of energy of an electron in the external field, or the drag of the electron, is defined according to Eq. (2.3.12), where the integral is taken over by Σ_ϵ.

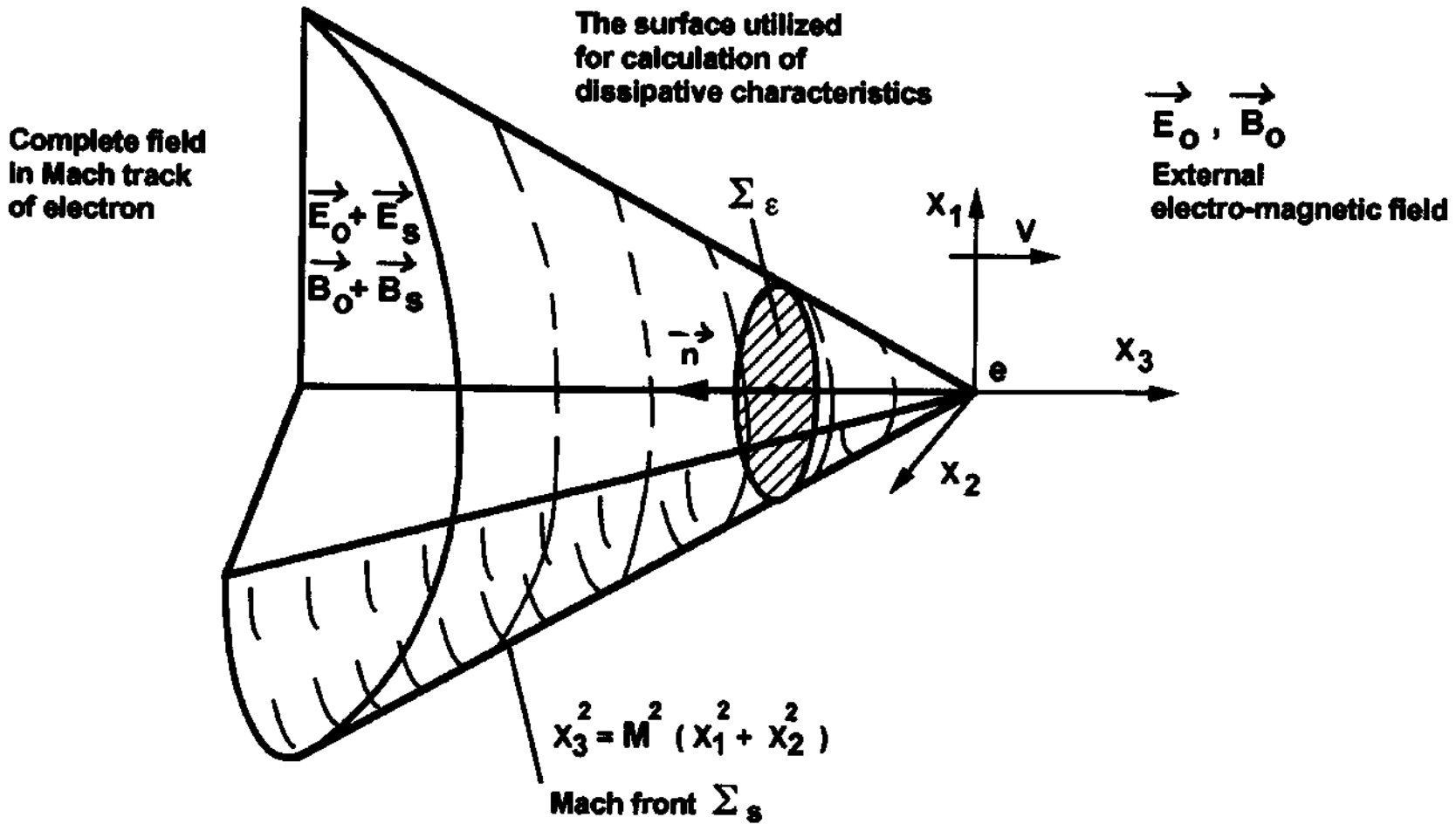

FIG. 12. The three-dimensional Mach front picture of an electron moving in a medium with a speed exceeding the phase speed of light.

At the Σ_ϵ surface we choose the small circular cross section of the Mach cone at $x_3=-\epsilon$ (see Fig. 12).

Electrostriction and magnetostriction effects are ignored here. Substituting Eqs. (3.1.1), (2.1.1), and (2.1.2) into Eq. (2.3.12), and calculating the corresponding surface integrals according to the rule of Γ integration when $\epsilon\to 0$, we obtain

$$\Gamma_i = e\mathbf{E}_{0i} \quad (i=1,2,3). \tag{3.1.2}$$

We omit the cumbersome calculations of all surface integrals and show only the calculation of D_3 (the force is directed along the axis of motion). In this case, we have

$$\Gamma_3 = \lim_{\epsilon\to 0} \frac{1}{2} \int_{\Sigma_\epsilon} (\mathbf{D}_1\mathbf{E}_1 + \mathbf{D}_2\mathbf{E}_2 + \mathbf{B}_1\mathbf{H}_1 - \mathbf{B}_2\mathbf{H}_2 - \mathbf{D}_3\mathbf{E}_3 - \mathbf{B}_3\mathbf{H}_3)\, d\Sigma. \tag{3.1.3}$$

By means of the rules of Γ integration, this integral can be reduced to

$$\Gamma_3 = -\lim_{\epsilon\to 0} e\mathbf{E}_{03}\epsilon \int_0^\epsilon \frac{\tau\, d\tau}{(\epsilon^2-\tau^2)^{3/2}} = e\mathbf{E}_{03}. \tag{3.1.4}$$

We note that the external field is considered in the coordinate system attached to the relativistic electron; alteration to the laboratory system is made by Lorentz's transformations. Formally, Eq. (3.1.2) coincides with corresponding expressions for a stationary electron.

B. One-dimensional, semi-infinite chain of superluminal electrons

Let another electron e_1 be situated inside the Mach cone of the first electron e_0 which moves with a superluminal velocity $V>a$. (Indices 0 and 1 are introduced here for the convenience of differentiation of these particles only.) For e_1 the external field will now be the field of electron e_0. Therefore, if both charges move along one axis, then on the axis $\mathbf{B}=0$, according to Eq. (2.1.2), let the value z be the distance between the particles. According to Eqs. (2.1.1) and (3.1.2), the force acting on the charge e_1 is:

$$F_1(z) = \frac{e_0 e_1 M^2}{2\pi\epsilon' z^2}, \tag{3.2.1}$$

where

$$M^2 = \frac{V^2/a^2-1}{1-V^2/c^2} \quad (M>0).$$

Equation (3.2.1) is the generalization of Coulomb's law. One can see from Eq. (3.2.1) that the rear electron e_1 is always attracted to the frontal electron e_0 when $\mathbf{V}>a$. In this case, there is no reaction of e_1 on e_0.

Let us consider the behavior of a one-dimensional, semi-infinite chain of superluminal electrons equidistantly separated by the interval b at the initial instant. In this case, forces exist directed only along the axis of the chain; we denote by f_{mn} the force acting on the mth electron, and due to the nth electron $(n<m)$, the resultant force acting on the mth electron is

$$F_m = \sum_{n=0}^{m-1} f_{mn}. \tag{3.2.2}$$

According to Eqs. (3.2.1) and (3.2.2), at the initial instant, we obtain

$$F_m(b) = \frac{e^2M^2}{2\pi\epsilon' b^2} \sum_{n=0}^{m-1} (n+1)^{-2}. \tag{3.2.3}$$

As is known,[79]

$$1 \leqslant \sum_{n=0}^{m-1} (n+1)^{-2} < \frac{\pi^2}{6}. \tag{3.2.4}$$

Hence,

$$F_1(b) \leqslant F_m(b) < \frac{\pi^2}{6} F_1(b). \tag{3.2.5}$$

From Eq. (3.2.5) it follows that for any m, the forces $F_m(b)$ differ little from F_1. Therefore, one can obtain a simple estimate of the deformation of a chain system by considering the motion of a single electron e_1 in the field produced by e_0.

Taking Eq. (3.2.1) into account, the relativistic equation of motion of electron e_1 in the moving coordinate system has the form[70–73]

$$\frac{d^2z}{dt^2} = \frac{e^2(\mu\epsilon V^2/c^2 - 1)}{2\pi\epsilon' m_0(1 - V^2/c^2)z^2}\left[1 - \frac{1}{c^2}\left(\frac{dz}{dt}\right)^2\right]^{3/2}. \tag{3.2.6}$$

First, we limit ourselves to the case of small relative particle velocities where $(1/c^2)(dz/dt)$ may be neglected in Eq. (3.2.6). Solving Eq. (3.2.6) for the following initial conditions,

$$z = -b \quad \text{and} \quad \frac{dz}{dt} = 0 \quad \text{at} \quad t = 0,$$

we obtain the solution

$$tK^{1/2} = b^{1/2}(-z)^{1/2}(z+b)^{1/2} + b^{3/2} \arcsin\left(1 + \frac{z}{b}\right)^{1/2}, \tag{3.2.7}$$

where

$$K = \frac{e^2(V^2/c^2 - \epsilon^{-1})}{\pi\epsilon_0 m_0(1 - V^2/c^2)} \quad (\mu = 1 \text{ for dielectrics}).$$

Let us estimate the time τ that is necessary for e_1 to approach e_0 for a very short distance. In this way, a dense system of two electrons is formed; quantum interactions are essential in this dense system, just as in a solid.

Substituting $z = 0$ into the solution, Eq. (3.2.7). we obtain the time for joining two electrons

$$\tau = \frac{\pi b^{3/2}}{2K^{1/2}}. \tag{3.2.8}$$

We note that quantities b. t. and τ are considered in the coordinate system fixed at the first electron. Using Lorentz transformation and the laboratory frame.

$$b' = b(1 - V^2/c^2)^{1/2}, \quad t' = t(1 - V^2/c^2)^{-1/2},$$

we obtain from Eq. (3.2.8)

$$(\tau')^2 = \frac{\pi^3 \epsilon_0 m_0 (b')^3}{4e^2(1 - V^2/c^2)^{3/2}(V^2/c^2 - \epsilon^{-1})}. \tag{3.2.9}$$

The dependence by τ' on V^2/c^2 for a dielectric material is shown in Fig. 13. As we can see, the distance between the two electrons contracts most substantially in a narrow region of energies (velocities) of the particles, where τ' is small. For $V^2/c^2 = (3+2\epsilon)/5\epsilon$, the time of condensation τ' takes the minimum value

$$\tau''_m = \frac{c_\pi (b')^{3/2}}{(1 - \epsilon^{-1})^{5/4}}, \tag{3.2.10}$$

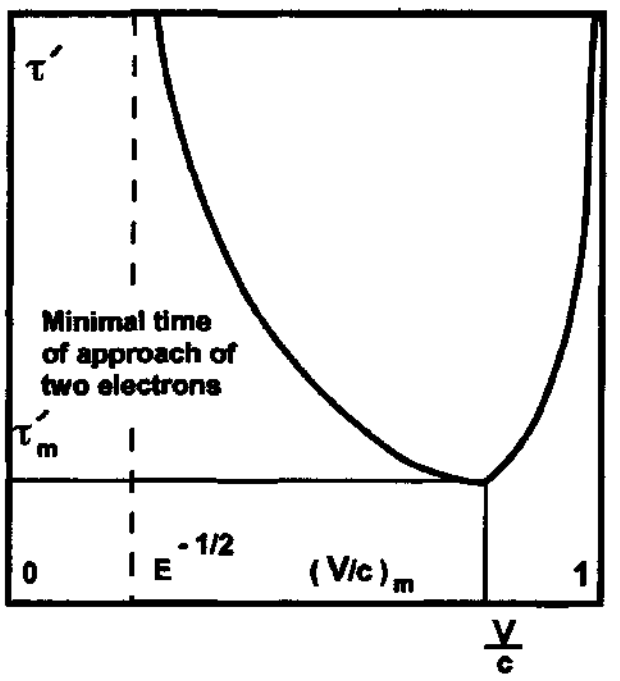

FIG. 13. Dependence of the laboratory time τ' for the mutual approach of two relativistic electrons at the velocity v/c.

where

$$c_m = \frac{(5^{5/4}\pi)^{3/2}\epsilon_0^{1/2} m_0^{1/2}}{12^{3/4} e}.$$

For an electron, $c_m = 6.437 \times 10^{-2}\ \mathrm{m}^{-3/2}\ \mathrm{s}$.

Hence, a chain of superluminal electrons condenses to a solidlike state during a time span τ' defined by Eq. (3.2.9). For instance, for $b' = 1\ \mu\mathrm{m}$ (on the order of the distance between electrons in pulsed electron beams), we obtain $\tau'_m \sim 10^{-10}$ s. This means that electron plasma clusters form at a depth on the order of 1 mm beneath the surface of an irradiated material.

C. Electron beams

As shown, relativistic electron beams exhibit the mechanism for self-compression. Since time T, for which the formulation of the problem remains valid is small, this mechanism can manifest itself only for high-density beams (small b'). From Eq. (3.2.10) the necessary particle density in the initial beam can be estimated as follows:

$$n_0(b')^3 > c_m^2(1 - \epsilon^{-1})^{-5/2} T^{-2}. \tag{3.3.1}$$

Quantity T is the time of run of the directed beam of superluminal electrons in a medium and is determined by the interplay of two factors: the deceleration of electrons to the phase speed of light in the medium, and the losses due to excitation and ionization of the fixed electrons of the material medium. A more precise value of critical density can be obtained from Eq. (3.2.9).

Consideration of the spatial distribution of electrons in a beam shows that forces acting inside the system are presumably directed along the axis of motion, but forces are also directed toward the boundary of the Mach cone. However, the latter forces are substantial only for boundary electrons, and in the far zone these forces are balanced by the action of other superluminal electrons. Moreover, dispersion of particle energies in a beam induces a Lorentz force, which depends on the relative velocity of motion.

It follows that the effect of self-compression can be observed experimentally when electron beams pass through a material, the thickness of which is smaller than the deceleration length. The initial density can be defined by Eq. (3.3.1), where T is the time of electron motion in the material.

Decrease of the pulse duration for self-compression of a beam can be estimated directly, if the initial duration of the pulse is smaller than T (otherwise, a series of local zones of large densities are created, and the initial pulse duration is not transformed). For example, in a dielectric 1 mm thick, initial density on the order of 10^{22} m^{-3}, is necessary in order to considerably decrease the pulse duration of a beam with a particle energy of 1 MeV.

The estimated value of the particle density is somewhat higher than the mean densities reached in electron accelerators. However, in small volumes (as compared to the dimensions of a beam) this density can be reached due to the inhomogeneities in the distribution of electrons in a beam and the avalanche of secondary ionized electrons.

IV. STEADY SUPERSONIC MOTION OF AN INFINITE THIN WEDGE

A. Equations for the steady plane problem of the theory of elasticity

For the plane problem, Lamé equations of the dynamic theory of elasticity are as follows:

$$\frac{\partial^2\Phi_i}{\partial x_1^2}+\frac{\partial^2\Phi_i}{\partial x_2^2}=\frac{1}{c_i^2}\frac{\partial^2\Phi_i}{\partial t^2} \quad (i=1,2), \tag{4.1.1}$$

where Φ_1 and Φ_2 are wave potentials; c_1 and c_2 are velocities of longitudinal and transverse waves in a medium; and x_1,x_2 is the system of coordinates connected with the medium. In the moving system of coordinates $x=x_1-\mathbf{V}t$, $y=x_2$, $t'=t$, connected with a wedge moving with speed $\mathbf{V}$, Eq. (4.1.1) in the steady case is

$$M_i^2\frac{\partial^2\Phi_i}{\partial x^2}=\frac{\partial^2\Phi}{\partial y^2} \quad (i=1,2), \tag{4.1.2}$$

where

$$M_i^2=\frac{\mathbf{V}^2}{c_i^2}-1>0.$$

Displacements, stresses, and velocities of the medium are expressed through the derivatives of wave potentials in the following way:

$$u_x=\frac{\partial\Phi_1}{\partial x}+\frac{\partial\Phi_2}{\partial y}-\mathbf{V}t,$$
$$u_y=\frac{\partial\Phi_1}{\partial y}-\frac{\partial\Phi_2}{\partial x}, \tag{4.1.3}$$

$$\sigma_{xx}=G(1+M_2^2-2M_1^2)\frac{\partial^2\Phi_1}{\partial x^2}+2G\frac{\partial^2\Phi_2}{\partial x\,\partial y},$$
$$\sigma_{yy}=G(M_2^2-1)\frac{\partial^2\Phi_1}{\partial x^2}-2G\frac{\partial^2\Phi_2}{\partial x\,\partial y}, \tag{4.1.4}$$

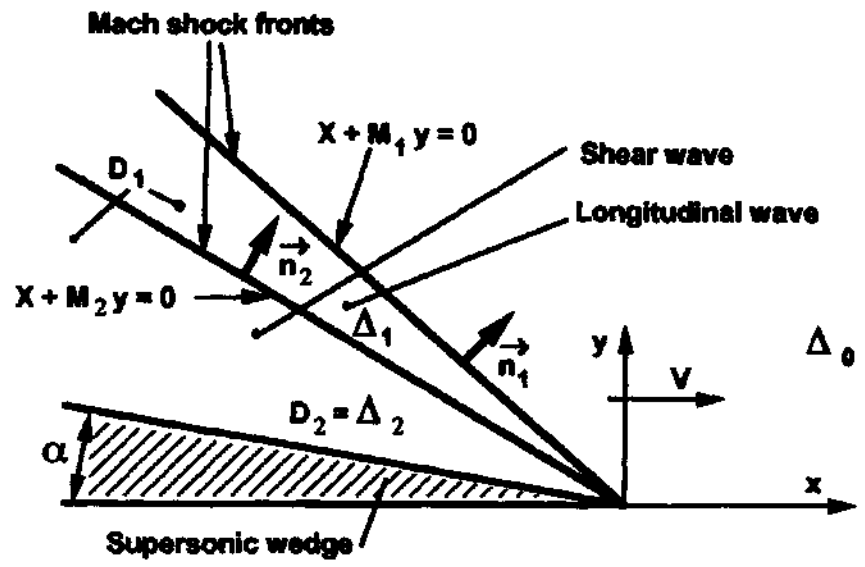

FIG. 14. The perturbation zone of a supersonic, two-dimensional wedge moving in an elastic solid.

$$\sigma_{xy}=2G\frac{\partial^2\Phi_1}{\partial x\partial y}+G(M_2^2-1)\frac{\partial^2\Phi_2}{\partial x^2},$$
$$v_x=\frac{\partial u_x}{\partial t}=-\mathbf{V}\left(1+\frac{\partial^2\Phi_1}{\partial x^2}+\frac{\partial^2\Phi_2}{\partial x\,\partial y}\right), \tag{4.1.5}$$
$$v_y=\frac{\partial u_y}{\partial t}=-\mathbf{V}\left(\frac{\partial^2\Phi_1}{\partial x\,\partial y}-\frac{\partial^2\Phi_2}{\partial x_2}\right).$$

Here u_x and u_y are displacements; σ_{xx}, σ_{xy}, and σ_{yy} are stresses; M_1 and M_2 are modified Mach numbers; and G is the shear modulus of the elastic medium.

Normal and tangent components of velocity, v_n and v_t, on a plane are expressed as follows:

$$v_n=v_in_i, \quad v_t=v_it_i \quad (i=x,y), \tag{4.1.6}$$

where n_i and t_i are respective components of a normal and tangent unit vector. The general solution to Eq. (4.1.2) is

$$\Phi_i=\varphi_i(x-M_iy)+\psi(x+M_iy) \quad (i=1,2), \tag{4.1.7}$$

where φ_i and ψ_i are arbitrary functions.

B. General solution to the problem of supersonic motion of an infinite thin wedge

First, let us consider a special case of the problem of the motion of a wedge with angle, α, as $l\to\infty$. The boundary conditions, Eqs. (2.2.1) and (2.2.2), along $y+\delta x=0$, $x<0$ are

$$v_n=0, \quad \sigma_{tn}=F(\sigma_n,v_t) \quad \delta=\tan\alpha, \tag{4.2.1}$$

where normal and tangent vectors are:

$$\mathbf{n}=\{\delta(1+\delta^2)^{-1/2}, \quad (1+\delta^2)^{-1/2}\},$$
$$\mathbf{t}=\{-(1-\delta^2)^{-1/2}, \quad \delta(1-\delta^2)^{-1/2}\}. \tag{4.2.2}$$

The wave potential Φ_i differs from zero in the corresponding area D_i situated between the surface of the wedge, $y+\delta x=0$, and the corresponding Mach line, $x+M_iy=0$, for the upper half-plane (Fig. 14). The Mach lines are the shock waves on which the laws of conservation of mass and momentum should be met. The wedge is considered thin, i.e., when the condition for the hypervelocity flow past a thin airfoil is satisfied,

$$\delta<\frac{1}{M_2}<\frac{1}{M_1}. \tag{4.2.3}$$

This means that each characteristic line of the corresponding family crosses the wedge surface only at one point and, therefore, the rectilinear shock waves are attached to the wedge vertex. Such a condition is analogous to forming a shock wave by a wedge in gas dynamics, and the mathematical problem is analogous to the problem of the flow of a supersonic gas around a thin wedge.[80,81]

Let Δ_0 be the undisturbed domain of an elastic body, Δ_1 the domain in which only Φ_1 does not equal zero, and Δ_2 the domain in which both Φ_1 and Φ_2 are not zero. In each of these domains, ρ_0, ρ_1, and ρ_2, $\mathbf{v}^{(0)}$, $\mathbf{v}^{(1)}$, and $\mathbf{v}^{(2)}$, and $\sigma_{ij}^{(0)}$, $\sigma_{ij}^{(1)}$, and $\sigma_{ij}^{(2)}$ are the densities, velocities, and stresses of the medium, respectively. The laws of conservation on the Mach lines follow.

(i) Along $x+M_1y=0$, with normal and tangent vectors,

$$\mathbf{n}=\{(1+M_1^2)^{-1/2},M_1(1+M_1^2)^{-1/2}\},$$

$$\mathbf{t}=\{-M_1(1+M_1^2)^{-1/2},(1+M_1^2)^{-1/2}\},$$

we obtain

$$\rho_0\mathbf{v}_{n1}^{(0)}=\rho_1\mathbf{v}_{n1}^{(1)}, \tag{4.2.4}$$

$$\sigma_{n1}^{(0)}-\sigma_{n1}^{(1)}=\rho_1\mathbf{v}_{n1}^{(1)}(\mathbf{v}_{n1}^{(0)}-\mathbf{v}_{n1}^{(1)}), \tag{4.2.5}$$

$$\sigma_{n1}^{(0)}-\sigma_{tn1}^{(1)}=\rho_1\mathbf{v}_{n1}^{(1)}(\mathbf{v}_{t1}^{(0)}-\mathbf{v}_{t1}^{(1)}). \tag{4.2.6}$$

(ii) Along $x+M_2y=0$, with normal and tangent vectors,

$$\mathbf{n}=\{(1+M_2^2)^{-1/2},M_2(1+M_2^2)^{-1/2}\},$$

$$\mathbf{t}=\{-M_2(1+M_2^2)^{-1/2},(1+M_2^2)^{-1/2}\},$$

we obtain

$$\rho_1\mathbf{v}_{n2}^{(1)}=\rho_2\mathbf{v}_{n2}^{(2)}, \tag{4.2.7}$$

$$\sigma_{n2}^{(1)}-\sigma_{n2}^{(2)}=\rho_2\mathbf{v}_{n2}^{(2)}(\mathbf{v}_{n2}^{(1)}-\mathbf{v}_{n2}^{(2)}), \tag{4.2.8}$$

$$\sigma_{tn2}^{(1)}-\sigma_{tn2}^{(2)}=\rho_2\mathbf{v}_{n2}^{(2)}(\mathbf{v}_{t2}^{(1)}-\mathbf{v}_{t2}^{(2)}). \tag{4.2.9}$$

Let us express the components of the velocity and stresses in Eqs. (4.2.4)–(4.2.9) through the derivatives of $\varphi_i(\xi)$ and $\psi_i(\xi)$ using Eqs. (4.2.6)–(4.2.9). As a result, we obtain

$$\varphi_1''(\xi)\equiv 0, \quad \varphi_2''(\xi)\equiv 0, \tag{4.2.10}$$

$$\rho_2=\rho_1=\rho_0[1+(1+M_i^2)\psi_1''(0)]^{-1}, \tag{4.2.11}$$

$$\begin{aligned}\mathbf{v}_x&=-\mathbf{V}[1+\psi_1''(x+M_1y)+M_2\psi_2''(x+M_2y)],\\ \mathbf{v}_y&=-\mathbf{V}[M_1\psi_1''(x+M_1y)-\psi_2''(x+M_2y)]\end{aligned} \tag{4.2.12}$$

$$\sigma_{xx}/G=(1+M_2^2-2M_1^2)\psi_1''(x+M_1y)+2M_2\psi_2''(x+M_2y),$$

$$\sigma_{yy}/G=(M_2^2-1)\psi_1''(x+M_1y)-2M_2\psi_2''(x+M_2y), \tag{4.2.13}$$

$$\sigma_{xy}/G=2M_1\psi_1''(x+M_1y)+(M_2^2-1)\psi_2''(x+M_2y).$$

In particular, on the wedge surface $y+\delta x=0$, according to Eqs. (4.2.7), and (4.2.8), we obtain

$$\mathbf{v}_n=-\mathbf{V}(1+\delta^2)^{-1/2}[\delta+(\delta+M_1)\psi_1''+(\delta M_2-1)\psi_2''], \tag{4.2.14}$$

$$\begin{aligned}\mathbf{v}_t&=-\mathbf{V}(1+\delta^2)^{-1/2}[(M_1\delta-1)\psi_1''-(\delta+M_2)\psi_2''-1],\\ \sigma_n&=G(1+\delta^2)^{-1}\{2(\delta M_2-1)(M_2+\delta)\psi_2''\\ &\quad+[(1+M_2^2-2M_1^2)\delta^2+4M_1\delta+M_2^2-1]\psi_1''\}\end{aligned} \tag{4.2.15}$$

$$\begin{aligned}\sigma_{tn}&=G(1+\delta^2)^{-1}\{2(M_1+\delta)(M_1\delta-1)\psi_1''\\ &\quad+[(M_2^2-1)\delta^2-4M_2\delta-M_2^2+1]\psi_2''\},\end{aligned}$$

where the function arguments $\psi_1(\xi_1)$ and $\psi_2(\xi_2)$ are $\xi_1=y(M_1\delta-1)/\delta$ and $\xi_2=y(M_2\delta-1)/\delta$.

Equations (4.2.12) and (4.2.13) constitute a general solution of the problem; the form of the functions $\psi_1(\xi_1)$ and $\psi_2(\xi_2)$ is determined by two conditions on the surface of the wedge.

Let us adduce the full account of the results of solving the problem when the condition $\sigma_{tn}=f\sigma_n$, where f is an arbitrary constant, is met on the surface of the wedge. Applying Eq. (4.2.14), we get from Eq. (4.2.1)

$$(1-\delta M_2)\psi_2''-(\delta+M_1)\psi_1''=\delta. \tag{4.2.16}$$

Here, the argument of functions $\psi_i(\xi_i)$ on the straight line, $y+\delta x=0$, as well as in Eqs. (4.2.14) and (4.2.15), is $\xi_i=y(M_i\delta-1)/\delta$. From Eqs. (4.2.2) and (4.2.15), we obtain

$$\begin{aligned}&\{2(M_1+\delta)(M_1\delta-1)-f[(1+M_2^2-2M_1^2)\delta^2+4M_1\delta\\ &\quad+M_2^2-1]\}\psi_1''+[(M_2^2-1)\delta^2-4M_2\delta+1-M_2^2\\ &\quad-2f(\delta M_2-1)(M_2+\delta)]\psi_2''=0.\end{aligned} \tag{4.2.17}$$

The solution of Eqs. (4.2.16) and (4.2.17) follows:

$$\begin{aligned}\psi_1''(\xi)&=-\delta\mathbf{A}^{-1}[(M_2^2-1)\delta^2-4M_2\delta+1-M_2^2\\ &\quad-2f(\delta M_2-1)(M_2+\delta)],\\ \psi_2''(\xi)&=\delta\mathbf{A}^{-1}\{2(M_1+\delta)(M_1\delta-1)\\ &\quad-f[(1+M_2^2-2M_1^2)\delta+4M_1\delta+M_2^2-1]\},\end{aligned} \tag{4.2.18}$$

where

$$\begin{aligned}\mathbf{A}&=(\delta+M_1)[(M_2^2-2M_1M_2-1)\delta^2+2(M_1-M_2)\delta-M_2^2\\ &\quad-1]-f(1-\delta M_2)[(M_2^2-2M_1^2-1)\delta^2\\ &\quad+2(M_1-M_2)\delta+M_2^2-2M_1M_2-1].\end{aligned}$$

It is also necessary to take $\psi_1''\equiv 0$ and $\psi_2''\equiv 0$ in Δ_0 and $\psi_2''\equiv 0$ in Δ_1.

C. Superthin wedge without friction

In the solution of Sec. IV B the value of f is assumed to be known, although such information concerning the motion of plasma wedges in a solid is not available. From Eqs. (4.2.18), one can see that f has a considerable effect

on the velocity and stresses only when it is close to unity, i.e., in the expansion of the solutions in Eqs. (4.2.18) into a power series of the form

$$\psi_i'' = \sum_{n=0}^{\infty} \alpha_{in} f^n.$$

Here coefficients α_{i1} are small in comparison to α_{i0}; therefore, the simplest solution of the problem in the limiting case of zero friction, when $f=0$, is of interest. This solution allows us to obtain effective estimates.

We shall confine ourselves to the case of superthin wedges, for which the following conditions are fulfilled:

$$\delta \ll \frac{1}{M_2} \quad \text{and} \quad \delta \ll \frac{1}{M_1}. \tag{4.3.1}$$

The solutions, Eqs. (4.2.18), for a superthin wedge, are reduced to

$$\psi_i'' = \frac{(1-M_2^2)\delta}{M_1(1+M_2^2)}, \quad \psi_2'' = \frac{2\delta}{1+M_2^2}. \tag{4.3.2}$$

Velocity and stress components in this case are equal to

$$\mathbf{v}_x = -\mathbf{V}(1+\psi_1''+M_2\psi_2''), \quad \mathbf{v}_y = \mathbf{V}(\psi_2''-M_1\psi_1''), \tag{4.3.3}$$

$$\begin{aligned} \sigma_{xx} &= \mu(1+M_2^2-2M_1^2)\psi_1'' + 2\mu M_2\psi_2'', \\ \sigma_{yy} &= \mu(M_2^2-1)\psi_1'' - 2\mu M_2\psi_2'', \\ \sigma_{xy} &= 2\mu M_1\psi_1'' + \mu(M_2^2-1)\psi_2'', \end{aligned} \tag{4.3.4}$$

where ψ_1'' is given by Eqs. (4.3.2) in Δ_1, $\psi_2'' = 0$ in Δ_1, and ψ_1'' and ψ_2'' are given by Eqs. (4.3.2) in Δ_2.

Density in the disturbed regions is determined by the expression

$$\rho_2 = \rho_1 = \rho_0\left(1+\frac{(M_2^2-1)(M_1^2+1)\delta}{M_1(1+M_2^2)}\right). \tag{4.3.5}$$

Normal and tangent stresses on the surface of the wedge in this limiting case are

$$\sigma_n = -\frac{\mu\delta[(M_2^2-1)^2+4M_1M_2]}{M_1(1+M_2^2)}, \quad \sigma_{in}=0. \tag{4.3.6}$$

Similarly, the case of the arbitrary shape of a wedge can be considered. The theory of cutting solid materials by high-power beams of elementary particles has recently been constructed,[47,82–84] taking into account the motion and position of a target.

V. DECELERATION OF THE FINITE WEDGE

A. Drag and dissipation of the energy of a wedge moving with supersonic speed in an elastic medium

Solutions of the plane problem of the infinite thin wedge presented in Sec. IV hold for the domain consisting of two characteristic triangles resting on the contact surface of a wedge of length l (see Fig. 9). This fact helps to determine energy dissipation and forces affecting the supersonic body without solving the problem as a whole.

Let us consider the plane problem of a cavity, at the end of which a moving supersonic wedge presses the body for a certain finite period. The length of the cavity is assumed to be much larger than the length of the wedge; the surface of the cavity is assumed to be free (the effect of the substance that may be present in the cavity outside the wedge is neglected). These conditions allow us to place zero disturbances at infinity. Choose the surface of integration Σ consisting of Σ_2, Σ_0, and Σ_w, as shown in Fig. 15, where Σ_2 is situated at an infinite distance from the wedge; Σ_0 is the free surface of the cavity; and Σ_w is the surface of the wedge contact with the medium. The Γ integral over this surface will provide the energy dissipation of the finite wedge, flowing into shock waves on Mach lines; the whole surface of the Γ integration embraces all singular surfaces.

The contribution to the Γ integrals over Σ is made only by Σ_w. Therefore, Eqs. (2.3.11) in the moving system of coordinates connected with the wedge will have the following form:

$$\Gamma_x = \int_{\Sigma_w} [(U'+\tfrac{1}{2}\rho \mathbf{v}_i'\mathbf{v}_i')n_x - \sigma_{ij}u_{i,x}n_f]\,d\Sigma$$

$$(i,j,k=x,y,z) \tag{5.1.1}$$

$$(\mathbf{v}' = \mathbf{v}_i + \mathbf{V}_i, \quad \mathbf{u}_i' = \mathbf{u}_i + \mathbf{V}_i t),$$

where $\mathbf{V}_i$ is the component of the wedge velocity vector and $\mathbf{V}=\{\mathbf{V},0\}$ and U' is the specific energy of the deformations.

It is easy to see that the second term in Eq. (5.1.1) is the sum of the surface forces acting on the rigid wedge. Let us label this term R_x. Then Eq. (5.1.1) becomes

$$\Gamma_x = W_x + R_x, \tag{5.1.2}$$

where W_x is the change of the internal energy of the medium expressed by the first term.

Let us calculate W_x and R_x in an explicit form for the simple case of the superthin symmetric wedge without friction. Let us use the solutions in Eqs. (4.3.2), (4.3.3), and (4.3.6) and the following expression:

$$U' = \tfrac{1}{4}\sigma_{ij}(u_{i,j}'+u_{j,i}') = [(1+\nu)\sigma_{ij}\sigma_{ij} - \nu\sigma_{ii}\sigma_{jj}]/2E, \tag{5.1.3}$$

for a linear-elastic medium, where ν is Poisson's ratio and E is Young's modulus. We obtain

$$W_x = \frac{FE\delta^3 l}{4(1+\nu)^2} \quad (W_y=0), \tag{5.1.4}$$

where

$$\begin{aligned} F = M_1^{-2}(1+M_2^2)^{-2}\{&[4M_1M_2+(1-M_2^2)^2]^2 \\ &+4[M_1M_2+(1-M_2^2)(1+M_2^2-2M_1^2]^2 \\ &+2M_1^2(1+\nu)(1+M_2^2)^3+2(1+\nu)(1+M_2^2) \\ &\times(2M_1M_2+1-M_2^2)\}. \end{aligned}$$

Further calculations give the following results:

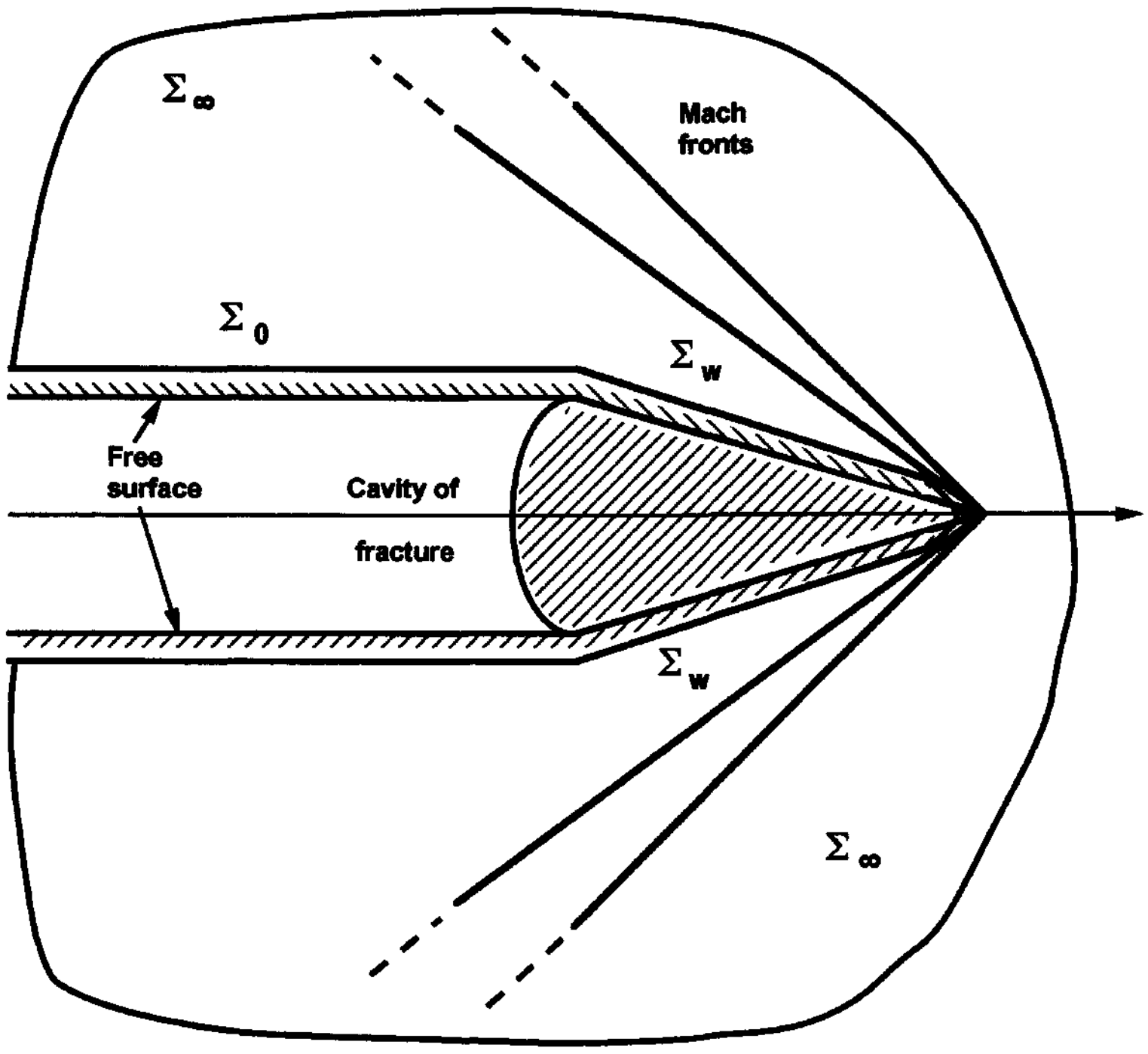

FIG. 15. Steady-state supersonic motion of a finite wedge.

$$R_x=\frac{-BE\delta^2 l}{1+\nu}=-2BG\delta^2 l$$
$$R_y=0, \tag{5.1.5}$$

where

$$B=\frac{(M_2^2-1)^2-4M_1M_2}{M_1(1-M_2^2)}.$$

Comparison of Eqs. (5.1.4) and (5.1.5) show that at small angles of the wedge opening, work spent to increase the internal energy of a solid W_x is small in comparison with work spent to decelerate the wedge R_x. Thus, the dissipative characteristics of the process of motion of the thin supersonic wedge are determined by the drag of the wedge.

The formula for the drag,

$$R_x=-\int_{\Sigma_w}\sigma_{ij}u'_{i,x}n_j d\Sigma, \tag{5.1.6}$$

is applicable for any dimensions of the cavities formed at the fracture.

B. Deceleration of the finite wedge

Let us consider the motion of the wedge subjected only to the forces of inertia and drag in quasisteady approximation, i.e., assuming that the drag is given by Eq. (5.1.5). At the initial time, the wedge possessed momentum, $m\mathbf{V}_0$, where m is the linear mass of the wedge. The law of motion of the wedge is

$$m\frac{d\mathbf{V}}{dt}=R_x(\mathbf{V}), \tag{5.2.1}$$

with the initial condition $\mathbf{V}=V_0$ at $t=0$. The solution of Eq. (5.2.1) has the form

$$t=\frac{-m}{2G\delta^2 l}\int_{\mathbf{V}_0}^{\mathbf{V}}\frac{M_1(1+M_2^2)}{(M_2^2-1)^2+4M_1M_2}d\mathbf{V}, \tag{5.2.2}$$

where $G=\rho_0 c_2^2$, and M_1 and M_2 are the following functions:

$$M_1=\sqrt{\mathbf{V}^2/c_1^2-1},\quad M_2=\sqrt{\mathbf{V}^2/c_2^2-1}.$$

For the most important limiting case, $\mathbf{V}/c_1\gg 1$, we obtain the following simple solution from Eq. (5.2.2):

$$\mathbf{V}=\mathbf{V}_0\exp\left(\frac{-2t\rho_0 c_1\delta^2 l}{m}\right). \tag{5.2.3}$$

The corresponding distance covered by the wedge for the period t equals

$$L(t)=\int_0^t \mathbf{V}\,dt=\frac{m\mathbf{V}_0}{2\rho_0\delta^2 c_1 l}\left[1-\exp\left(\frac{-2\rho_0 c_1 t\delta^2 l}{m}\right)\right]. \tag{5.2.4}$$

Because $m=\rho_w \delta l^2/2$, where ρ_w is the density of the wedge substance, from Eq. (5.2.4), we obtain

$$\frac{L_\infty}{l}=\frac{\rho_w \mathbf{V}_0}{4\delta\rho_0 c_1}. \tag{5.2.5}$$

Equation (5.2.5) gives the length of the crack formed due to supersonic motion of the wedge, the subsonic phase of motion being neglected.

Taking into account Eq. (4.3.1), we can also derive the following estimate:

$$\frac{L_\infty}{l}\gg\frac{\rho_w \mathbf{V}_0^2}{4\rho_0 c_1^2}. \tag{5.2.6}$$

It is used below.

VI. FORMATION OF CONDENSED ELECTRON-PLASMA CLUSTERS IN CRYSTALS (A COMPARATIVE ANALYSIS OF THE THEORETICAL AND EXPERIMENTAL RESULTS)

A. Preliminary remarks

The mechanical model of the supersonic cutting of the EFM in Secs. IV and V based on a qualitative analysis of the experimental observations was not associated with the quantitative characteristics of electron radiation. It is necessary to evaluate the model with respect to known fracture experiments and estimate the basic parameters of the condensed electron plasma clusters formed in the materials under study.

The orders of magnitudes used for further calculation are: $\tau=1$ ns, the irradiation intensity, $\Phi_0=10^{18}$ m^{-2}; the electron energy $E=10^{-13}$ J (1 MeV); the cross-sectional area of the specimen $S=5\times10^{-5}$ m^2; the specimen thickness $h_s=5\times10^{-4}$ m; the relativistic momentum of an electron

$$p=\sqrt{(E_0/c)^2-m_0^2c^2}=5\times10^{-22}\ N\times s;$$

material density $\rho_0=10^3$ kg/m^3; the speed of the longitudinal waves $c_1=10^3$ m/s; the atomic spacing $a=10^{-9}$ m; the ideal theoretical strength of the crystals $U=10^{11}$ J/m^3; the specific surface energy of the crystals $\gamma=1$ J/m^2, and the electron mass at rest $m_0=10^{-30}$ kg. The total momentum of a beam for a pulse is $P=10^{-9}$ N s; the mean value of the specific energy absorbed in a material $g=5\times10^7$ J/m^3; and the energy absorbed in a specimen for a pulse $\Delta A=1$ J. These numerical values are typical for experiments for fracturing ionic crystals.

These data show that the specific energy of a fracture is three orders smaller than the theoretical strength of crystals. However, if one assumes that all energy is spent to form one or two cracks, the surface energy is equal to 10^4 J/m^2; this magnitude is much greater than the surface energy. The mechanical model of supersonic fracture has removed the contradiction and, now, a physical mechanism of cluster formation using the electron beam self-compression effect needs to be estimated.

B. Ionization electrons

As mentioned above, the electron density necessary for considerable self-compression of primary electrons is substantially greater than the initial density of a beam.

However, irradiation induces considerable ionization of fixed electrons. According to experimental data,[30] the energy dissipation of fast electrons by ionization is characterized by the parameter, $-\partial E/\partial(\rho x)\simeq 2\times10^5$ eV m^2/kg, for kinetic energy E, from 0.1 to 100 MeV. Specific loss of energy per unit thickness is equal approximately to $k=5\times10^{-11}$ J/m for typical density ρ_0. Using the Bethe–Bloch formula, we obtain a quantity of the electrons η' per unit-thickness liberated by one fast electron,

$$\eta'=\frac{k}{I+E_i}, \tag{6.2.1}$$

where I is the ionization energy of a fixed electron (for many materials, it is equal approximately to 10 eV), and E_i is the liberated electron energy.

The magnitude E_i may approach 10 eV, too. (The corresponding velocities of electrons are $\mathbf{V}\sim10^5$–10^6 m/s for typical speeds of electron clusters in irradiated materials.) Hence, the mean density of the liberated electrons n_i, is equal to

$$n_i=\Phi_0\eta'=\frac{k\Phi_0}{I+E_i}=5\times10^{25}\ \text{m}^{-3}. \tag{6.2.2}$$

This value is more than the initial density of a relativistic beam n_0 by seven orders.

Even much greater densities of electron clusters are possible. For example, in anisotropic crystals having cleavage planes, there exist prevailing directions of motion of electron clusters along the cleavage planes.[12] Anisotropy of mechanical properties is explained by the atomic anisotropy of crystals; therefore, the ionization energy of an electron depends on the directions of motion. A considerable current of secondary electrons will probably be created on the cleavage planes of the material. Directed secondary currents can possibly be formed by the transference of a superluminal electron momentum to liberated electrons and the redistribution of the density of secondary electrons.

Obviously, the formation of clusters of secondary electrons is possible along all of the cleavage planes. An electron current passing through the weakest cleavage plane will have the form of a thin blade. The thickness of the blade d will be much less than the two other dimensions l.

An upper bound for the density of a blade-shaped cluster of secondary electrons ρ_w can be estimated, assuming that all ionized electrons are collected in a blade of dimensions $d\times l\times l$. We obtain

$$\rho_w<\rho_w^*=\frac{m_0 k h_s S\Phi_0}{dl^2(I+E_i)}. \tag{6.2.3}$$

Note that the specimen lengths are usually smaller than the distance that electrons move, at $\mathbf{V}_0=10^5$ m/s, during the time of fracture τ_f. (The latter is of the order of 0.1 μs.)

We use Eq. 6.2.3 to answer the question about the possibility of mechanical cutting by the liberated electrons. Substituting ρ_w^* into Eq. (5.2.6), assuming $L_\infty = h_s$, and using the relationship $d = 2l\delta$, we find

$$d^2 < \frac{k m_0 V_0 S \Phi}{2\rho_0 c_1 (I + E_i)} = 5 \times 10^{-11} \text{ m}^2. \tag{6.2.4}$$

Taking into consideration that the destruction of material continuity begins at approximately 10^{-10} m, we obtain

$$10^{-10} < d < 7 \times 10^{-6} \text{ m}. \tag{6.2.5}$$

The avalanche formation of secondary liberated electrons by relativistic electrons provides another possible mechanism of the self-condensation of electrons and nucleation of solid plasma clusters.

C. Parameters of clusters: Comparison of the theory with experimental data

Let us estimate other parameters of the condensed clusters of electron plasma using the following scheme for fracture: (i) The electron fracture of solids is performed by clusters that are formed by a κth part of liberated electrons in a specimen domain with characteristic lengths of the order of h_s; (ii) fracture is defined as a failure of the atomic bonds of the nearest lattice atoms, and we assume further that $d = 10^{-9}$ m in accordance with Eq. (6.2.5).

From Eq. (6.2.4), the mass density of a cluster of liberated electrons (and the density of the model wedge) is

$$\rho_w = \frac{\kappa m_0 k h_s^2 \Phi_0}{l d (I + E_i)}. \tag{6.3.1}$$

The unknown values l, δ, ρ_w, and k, are related by the equations of the mechanical model,

$$\frac{L_x}{l} = \frac{\rho_w V_0}{4\rho_0 c_1 \delta}, \tag{6.3.2}$$

$$d = 2l\delta. \tag{6.3.3}$$

and by the obvious inequalities of the same model.

$$\delta \ll \frac{c_1}{V_0} \sim 10^{-3}, \tag{6.3.4}$$

$$\frac{L_\infty}{l} \gg 1. \tag{6.3.5}$$

From Eqs. (6.3.1)–(6.3.5), we find the following estimates for electron clusters:

$$1\ \mu\text{m} \lesssim l \lesssim 50\ \mu\text{m}, \tag{6.3.6}$$

$$10^{-5} \lesssim \underline{\kappa} \lesssim 10^{-3}, \tag{6.3.7}$$

$$5 \times 10^{-4}\ \text{kg/m}^3 \lesssim \rho_w \lesssim 10^{-1}\ \text{kg/m}^3, \tag{6.3.8}$$

$$5 \times 10^{26}\ \text{m}^{-3} \lesssim n_w \lesssim 10^{29}\ \text{m}^{-3}, \tag{6.3.9}$$

$$10^1 \lesssim \frac{L_x}{l} \lesssim 10^3, \tag{6.3.10}$$

where n_w is the electron density in the cluster.

For the specimen thickness h_s much greater than h_0, the depth L_∞ of the electron fracture mode is proportional to the intensity Φ (an electron cluster is created in the strata of thickness h_0). From Eqs. (6.3.1) and (6.3.2), we have

$$L_\infty = \lambda \Phi, \quad \lambda = \frac{\kappa m_0 k l h_0^2 V_0}{2d^2 \rho_0 c_1 (I + E_i)}. \tag{6.3.11}$$

According to Eqs. (6.3.6)–(6.3.10) and the values of the parameters of the EFM, the coefficient, λ is of the order of 10^{-20} m^3, which agrees with the experiments. Hence, the theoretically derived dependence of L_∞ on Φ confirms the experimental data (see Fig. 4).

The estimate for l in Eq. (6.3.6) provides a sufficiently narrow range for the dimension of the cluster. The dimensions of the material inhomogeneities, which form a secondary electron cluster, are of the same order. This value is comparable with the lengths of material structural defects as dislocations, microcracks, and grains (in polycrystalline metals), but it is smaller than the macrocrack dimensions.

VII. CONCLUSION

The model suggested allows us to comprehend the main peculiarities specific to the electron fracture mode (EFM): namely, the quite brittle style of fracture, the independence of the threshold beam intensity of the primary cracks, and the supersonic velocity of the crack propagation. The model is quite simple and rather effective. Therefore, we anticipate that it will stimulate further research.

The basic idea of the theory presented is that the supersonic fracture process is accompanied by a very small amount of work to render a fracture. The invention of extremely thin hypervelocity beams of very great density will allow one to cut solids with minimum damage and energy spent to fracture. Achieving such an invention is physically possible according to this theory.

Besides relativistic electron beams of great density, beams of other elementary particles, e.g., protons and intense photon rays, can probably induce the same mode of fracture. Probably, this is valid also for giant laser beams in the nanosecond range; however, a great deal of experimental and theoretical work is required to achieve a full understanding of the EFM phenomenon.

ACKNOWLEDGMENTS

The work was partially supported by Florida International University. Helen Rooney typed the improved English version of the paper and edited the entire text. Larisa Cherepanov prepared the figures in this paper. The courtesy and support of the staff and faculty of the Department of Mechanical Engineering at Florida International University and especially the Chairperson, Professor M. A. Ebadian, are gratefully acknowledged.

[1] R. B. Oswald, IEEE Trans. Nucl. Sci., NS-13, 63 (1966).
[2] N. K. Atamanova, A. I. Melker, and I. L. Tokmakov, Fiz. Chim. Obrabotky Materialov 4, 29 (1976).
[3] M. Hirai, Y. Konde, T. Yoshinari, and M. Ueta, J. Phys. Soc. Jpn. 30, 1071 (1971).

[4] J. I. Perkin, E. Norrin, and D. W. Large, J. Phys. D **4**, 974 (1971).
[5] R. B. Oswald, J. Appl. Phys. **44**, 3563 (1973).
[6] T. Miyazaki and N. Taniguchi, Sci. Papers Inst. Phys. Chem. Res. **1**, 67 (1973).
[7] B. Steverding and F. P. Gibson, J. Phys. D **10**, 1683 (1977).
[8] R. M. Schmidt, J. Phys. Chem. Solids **39**, 375 (1978).
[9] R. M. White and R. H. Gobbet, J. Phys. D. 7, 2342 (1974).
[10] Y. Kondo, M. Hirai, and M. Ueta, J. Phys. Soc. Jpn. **33**, 151 (1972).
[11] D. I. Vaisburd and G. I. Gering, Fiz. Tverd. Tela **16**, 3178 (1974).
[12] I. N. Balichev and D. I. Vaisburd, Fiz. Tverd. Tela **17**, 1236 (1975).
[13] D. I. Vaisburd and I. N. Balichev, Pis'ma Zh. Tekh. Fiz. **1**, 531 (1975).
[14] G. I. Gering and A. N. Valiaev, Izv. Vysch. Uchebn. Zaved. SSSR Fiz. **5**, 104 (1974).
[15] I. N. Balichev, *The Fracture of Ionic Crystals by Nanosecond Electron Beams High Density* (Tomsk University Press, Tomsk, 1974).
[16] I. N. Balichev, D. I. Vaisburd, and G. I. Gering, Pis'ma Zh. Tekh. Fiz. **2**, 327 (1976).
[17] I. N. Balichev, D. I. Vasburd, and S. B. Maltis, Dokl. Acad. Nauk SSSR **241**, 1330 (1978).
[18] D. I. Vaisburd and I. N. Balichev, Pis'ma Zh. Eksp. Teor. Fiz. **15**, 537 (1972).
[19] D. I. Vaisburd, I. N. Balichev, and A. N. Valiaev, Izv. Acad. Nauk SSSR Ser. Fiz. **40**, 2404 (1976).
[20] D. I. Vaisburd, I. N. Balichev, and A. N. Valiaev, Izv. Acad. Nauk SSSR Ser. Fiz. **38**, 1281 (1974).
[21] D. I. Vaisburd, A. N. Valiaev, and G. I. Gering, in *Fizika i Chimia Ionnykh Cristallov* (Riga, 1975).
[22] A. A. Vorob'ev, *Mechanical and Heat Properties of Alkaline Halogen Crystals* (Vyschaya Shcola, Moscow, 1968).
[23] D. I. Vaisburd, G. I. Gering, and V. M. Kondrashov, Zh. Tekh. Fiz. **5**, 1971 (1976).
[24] J. Badian and J. Reffi, in *Deystviye Lazernogo Izlucheniya* (Mir, Moscow, 1968).
[25] B. W. Schumacher and R. C. Smith, in Advances in Rock Mechanics (Washington, 1974), Vol. 2, Part B.
[26] R. T. Avery and D. Keefe, IEEE Trans. Nucl. Sci. **NS-20**, 61 (1975).
[27] R. T. Avery and D. Keefe, IEEE Trans. Nucl. Sci. **NS-20**, 1391 (1973).
[28] A. A. Vorob'ev, *Damage Accumulation, Structure Degradation, and Minerals and Rocks Fracture* (Tomsk University Press, Tomsk, 1973).
[29] G. A. Mesiatz, A. S. Nasibov, and V. V. Kremnev, *Formation of High-Voltage Nano-Second Pulses* (Energia, Moscow, 1970).
[30] H. Frauenfelder and E. M. Henley, *Subatomic Physics* (Prentice-Hall, Englewood Cliffs, NJ, 1974).
[31] C. Kittel, *Introduction to Solid State Physics*, (Wiley, New York, 1967).
[32] W. M. Peffey, Appl. Phys. Lett. **10**, 171 (1967).
[33] G. P. Cherepanov and V. Z. Parton, in *Mekhanika v SSSR za 50 let* (Nauka, Moscow, 1972), Vol. 3.
[34] G. P. Cherepanov, *Mechanics of Brittle Fracture* (McGraw-Hill, New York, 1979).
[35] A. A. Borzykh and G. P. Cherepanov, Prob. Prochn. **8**. 16 (1980).
[36] A. I. Melker and I. L. Tokmakov, Fiz. Chim. Obrabotky Materialov **2**, 62 (1977).
[37] A. A. Borzykh and G. P. Cherepanov, Prikl. Mat. Mekh. **44**, 1120 (1980).
[38] A. A. Borzykh, Mekh. Tverd. Tela **6**, 178 (1979).
[39] D. I. Vaisburd and S. I. Kasatkin, Izv. Vysch. Uchebn. Zaved. SSSR Fiz. **7**, 142 (1978).
[40] B. Steverding, C. W. Austin, and A. H. Warkheister. J. Appl. Phys. **43**, 3217 (1972).
[41] B. Steverding and S. H. Lehnigk, J. Appl. Phys. **42**, 3231 (1971).
[42] G. I. Barenblatt and G. P. Cherepanov, Prikl. Mat. Mekh. **24**, 824 (1960).
[43] D. R. Curran, D. A. Shockey, and S. Winkler. Int. J. Fract Mech. **6**. 271 (1970).
[44] S. R. Winkler, D. A. Shockey, and D. R. Curran. Ref. **43**. **6**. 151 (1970).
[45] S. R. Winkler, in *Dynamic Crack Propagation*, edited by G. Sih (Noordhoff, Leyden, 1973).
[46] L. I. Mirkin, *Physical Fundamentals of Material Treatment by Laser Beams* (Moscow University Press, Moscow, 1975).
[47] G. P. Cherepanov, *Rock Fracture Mechanics in Drilling* (Nedra, Moscow, 1987).
[48] T. Ekobory, *Fracture and Strength Mechanics and Physics of Solids* (Metallurgia, Moscow, 1972).
[49] *Fracture*, edited by H. Liebowitz (Academic, New York, 1968–1972), Vols. 1–7.
[50] *Dynamic Crack Propagation*, edited by G. Sih (Noordhoff, Leyden, 1973).
[51] A. A. Vedenov and E. P. Velikhov, Zh. Eksp. Teor. Fiz. **20**, 1110 (1962).
[52] F. C. Perry, Appl. Phys. Lett. **17** (1970).
[53] F. Platzman and P. Volf, *Volny i Vzaimodeistvia v Plasme Tverdogo Tela* (Mir, Moscow, 1975).
[54] A. I. Melker, A. I. Michailov, and N. V. Zolotorevsky, Fiz. Tverd. Tela **21**, 1545 (1979).
[55] A. I. Melker, S. N. Romanov, and I. L. Tokmakov, Fiz. Chim. Obrabotky Materialov **2**, 18 (1979).
[56] S. I. Molovsky and A. D. Sushkev, *High-Power Electron and Ion Beams* (Energia, Leningrad, 1972).
[57] W. T. Sanders, Eng. Fract. Mech. **4**, 145 (1972).
[58] P. A. Cherenkov, Dokl. Akad. Nauk SSSR **20**, 451 (1934).
[59] P. A. Cherenkov, Dokl. Akad. Nauk SSSR **22**, 653 (1938).
[60] P. A. Cherenkov, Tr. Fiz. Inst. Akad. Nauk SSSR **2**, 3 (1944).
[61] S. I. Vavilov, Dokl. Akad. Nauk SSSR **2**, 457 (1934).
[62] I. E. Tamm and I. M. Frank, Dokl. Akad. Nauk SSSR **14**, 107 (1937).
[63] I. E. Tamm, J. Phys. USSR **1**, 439 (1939).
[64] A. A. Borzykh and G. P. Cherepanov, Zh. Eksp. Teor. Fiz. **51**, 59 (1980).
[65] G. P. Cherepanov, Prikl. Mat. Mekh. **31**, 476 (1967).
[66] G. P. Cherepanov, Prikl. Mat. Mekh. **41**, 399 (1977).
[67] G. P. Cherepanov, Eng. Fract. Mech. **14**, 39 (1981).
[68] G. P. Cherepanov, in *Computational Methods in the Mechanics of Fracture*, edited by S. Atluri, Russian ed. (Mir, Moscow, 1990), pp. 350–365.
[69] L. D. Landau and E. M. Lifshitz, *Electrodynamics of Continuum Media* (Gostekhizdat, Moscow, 1959).
[70] L. D. Landau and E. M. Lifshitz, *Classical Theory of Fields* (Pergamon, London, 1975).
[71] I. I. Goldenblat and S. V. Ul'ianov, *Introduction to the Theory of Relativity and Its Application to Novel Techniques* (Nauka, Moscow, 1979).
[72] V. G. Levich, *Course of Theoretical Physics* (Nauka, Moscow, 1969), Vol. 1.
[73] A. A. Sokolov and I. M. Ternov, *Relativistic Electrons* (Nauka, Moscow, 1974).
[74] B. M. Budak, A. A. Samarsky, and A. N. Tikhonov, *Sbornik Zadach po Matematicheskei Fizike* (Nauka, Moscow, 1972).
[75] J. Cole and J. Huth, J. Appl. Mech. **25**, 433 (1958).
[76] L. M. Milne-Thomson, *Theoretical Hydrodynamics* (St. Martin's, New York, 1960).
[77] S. M. Belotserkovsky and I. K. Lifanov, *Method of Discrete Vortices*, edited by G. P. Cherepanov (CRC, Boca Raton, FL, 1993), pp. 1–18.
[78] J. C. Maxwell, *Treatise on Electricity and Magnetism* (Cambridge University Press, Cambridge, 1864).
[79] G. B. Dwight, *Table of Integrals and Other Formulas* (Collier-MacMillan, New York, 1961).
[80] N. E. Kochin, I. A. Kibel, and N. V. Roze, *Theoretical Hydromechanics* (Nauka, Moscow, 1963), Vol. 2.
[81] R. Courant and K. O. Friedrichs. *Supersonic Flow and Shock Waves* (Wiley-Interscience. New York. 1948).
[82] G. P Cherepanov and V. A. Pinsker, Sov. Min. Sci. **6**, 90 (1987).
[83] G. P. Cherepanov and V. A. Pinsker, Strength Mater. **11**, 24 (1988).
[84] G. P. Cherepanov and V. A. Pinsker, Sov. Min. Sci. **12**, 107 (1989).